AN INVESTIGATION ON THE SEISMIC BEHAVIOR OF NAHRAIN DAM, TABAS, IRAN

A THESIS SUBMITTED TO
The GRADUATED SCHOOL OF NATURAL AND APPLIED SCIENCES
OF
MIDDLE EAST TECHNICAL UNIVERSITY

BY

MOHAMMAD D.K. SORKHABI

IN PARTIAL FULFILLMENT OF THE REQUIREMENTS FOR THE
DEGREE OF MASTER OF SCIENCE
IN
THE DEPARTMENT OF CIVIL ENGINEERING

APRIL 2004

Approval of the Graduate school of Natural and Applied Science s.

…………………………

Prof. Dr. Canan Toker
Director

I certify that this thesis satisfies all requirements as a thesis for the degree of Master of Science

…..……………………….
Prof. Dr. Erdal ÇOKCA
Head of Department

We certify that we have read this thesis and that in our opinion it is fully adequate, in scope and quality, as a thesis for the degree of Master of Science.

…………………………
Prof. Dr. M.Yener ÖZKAN
Supervisor

Examining Committee Members

Prof. Dr. Yıldız WASTI	………………………
Prof. Dr. M.Yener ÖZKAN	………………………
Prof. Dr. Erdal ÇOKCA	……………………….
Prof. Dr. Celal KARPUZ	……………………….
Assoc. Prof. Dr. Can BALKAYA	……………………….

ABSTRACT

AN INVESTIGATION ON THE SEISMIC BEHAVIOR OF NAHRAIN DAM, TABAS, IRAN

D.K. Sorkhabi, Mohammad

M.S. Department of Civil Engineering

Supervisors: Prof. Dr. M. Yener ÖZKAN

April 2004, 89 pages

This study is an evaluation on the seismic behavior of the Nahrain Dam, which is located in Khorasan province in the central part of Iran. The finite element method is used for the dynamic analysis of the dam. Using a slope stability computer program, the critical slip surface near the crest of the dam and the yield acceleration corresponding to this slip surface are determined. Static analysis was completed by using the finite element computer program SAP90 and SAP2000 in order to determine the stress conditions within the body of the dam prior to earthquake. The stresses obtained from this analysis were used in the assessment of the dynamic material properties of the dam. Two near by actual earthquakes were modified and used as input motions of different magnitudes. At the next step, the harvested data was used as input data for the program TELDYN to perform dynamic analysis. Permanent displacements under the scenario base motions were calculated by using the Newmark's method.

Keywords: Earthfill Dams, Embankment Dams, Dynamic Analysis, Permanent Displacement Method, Finite Element Method, Earthquakes.

öZ

İRAN TABAS, NAHRAİN BARAJININ SİSMİC DAVRANIŞI ÜZERİNE BİR İNCELEME

D.K.SORKHABI, MOHAMMAD

Yüksek Lisans Tezi, İnşaat Mühendisliği Bölümü

Tez Yöneticisi: Prof. Dr. M. Yener ÖZKAN

Nisan, 2004, 89 sayfa

Bu çalişmanın konusu, İran'in merkezi bölümünde, Horasan Vilayetinde yapılan Nahrain barajinin sismik davranışına ilişkin bir değerlendirmedir. Yapılan dinamik analizlerde sonlu elemanlar metodu kullanılmıştır.

İlk olarak baraj kretine yakın bölgedeki kiritik kayma yüzeyi ve ona karşılık gelen kritik ivme, bir şev stabilitesi bilgisayar programı yardımı ile belirlenmiştir. SAP 90 ve SAP2000 sonlu elemanlar programı kullanılarak barajın gövdesindeki deprem öncesi statik gerilmeler hesaplanmiştir. Bu gerilmelerden daha sonra barajı oluşturan malzemelerin dinamik özelliklerinin

belirlenmesinde yararlanılmıştır. Baraj yerine yakin iki gerçek deprem kaydı modifiye edlilerek senaryo depremleri olarak kullanılmışlardır. Bir sonraki aşamada, hazırlanan veriler, dinamik analiz sonlu elemanlar bilgisayar programi TELDYN'e girdi olarak dahil edilmek sureti ile dinamik analiz gerçekleşmiştir. Senaryo depremleri altında kritik kayma yüzeyinde beklenen kalıcı deplasmanlar Newmark yöntemi ile tahmin edilmiştir.

Anahtar Kelimeler **:** Toprak Dolgu Barajlar, Dolgu Barajlar, Dinamik Analiz, Kalıcı Deplasmanlar Metodu, Sonlu Elemanlar Metodu, Deprem.

TO MY WIFE

ACKNOWLEDGMENTS

I would like to express my gratitude to my thesis supervisor Prof. Dr. M. Yener ÖZKAN for his kind and wise guidance during preparation of the present thesis.

I would also like to thank to the ambassador of Islamic Republic of Iran in Ankara, H.E. Firouz Dowlatabadi for his kind support for preparing the necessary documents and reports from the Ministry of Electricity and Water Resources.

In addition, I would also to thank to Morteza Ali Mohammadianö Hamid Alimohammadian and Farrokh Rasouli for their assistance to prepare data and in computer related works.

Finally, I would like to thank to my family for their support throughout my study.

TABLE OF CONTENTS

LIST OF TABLES

LIST OF FIGURES

LIST OF SYMBOLS

$\Delta\sigma_x$	: Change at the normal stress in x-direction
$\Delta\varepsilon_x$	: Change at the normal strain in x-direction
$\Delta\sigma_{xy}$	: Change at the shear stress on xy plane
$\Delta\varepsilon_{xy}$	: Change at the shear strain on xy plane
$\Delta\sigma_y$	: Change at the normal stress in y-direction
$\Delta\varepsilon_y$	: Change at the normal strain in y-direction
$\sigma'_1, \sigma'_2, \sigma'_3$	: Principal stresses
σ'_m	: Mean effective stress
β_n	: N_{th} root of a period relation
ΔW	: Dissipated energy
σ_y	: Vertical earth pressure
λ	: Damping ratio
ρ	: Density
γ	: Shear strain
ε	: Standard error term
[C]	: Global damping matrix
[K]	: Global stiffness matrix
[M]	: Global mass matrix
A	: Constant
a_{ave}	: Average acceleration
a_b	: Acceleration of inclined plane
A_n, B_n	: Constants
a_{rel}	: Relative acceleration
a_y	: Yield acceleration
b	: Constant
d	: Closest horizontal distance to the fault

e	: Void ratio
E	: Young's modulus
E,F	: Moment arms
F_b	: Total force acting on sliding block
F_e	: Force acting on an element
FS	: Factor of safety
g	: Gravitational acceleration
G	: Shear modulus
G_{max}	: Maximum shear modulus
G_{sec}	: Secant shear modulus
h	: Height of the dam
J_0	: Bessel function
K	: Bulk modulus
K_2	: Parameter relating G_{max} and σ'_m
K_g	:Parameter used for determining maximum shear modulus
k_h	: Horizontal seismic coefficient
l	: Length of sliding surface
M	: Magnitude
m_{ib}	: Mass of sliding block
m_{ie}	: Mass of element
M_s	: Surface wave magnitude
M_w	:Moment magnitude
ng	: Exponent used for determining maximum shear modulus
P_a	: Atmospheric pressure
R	: Radius of sliding surface
s	: Shear strength
t	: Time

u	: Displacement
V_s	: Shear wave velocity
W	: Maximum strain energy
W	: Weight

Chapter I

Introduction

1 .1 General

Due to environmental problems and rapid increase of world population, water shortage has become a major and complicated problem in the world especially in the Middle East. On the other hand, water control and assured water availability of appropriate quality have become essential requirements for continuing economic and social development. To achieve this goal large numbers of dams were constructed all over the world. Most of these dams are situated in the seismic zones. Since scale of the dam projects are very large and the process of the construction is almost irreversible, dam safety evaluation is a major engineering concern.

Earthquakes can affect embankment dams by causing any of the following:

- Settlement and cracking of the embankment, particularly near the crest of the dam|;
- Reduction of freeboard due to settlement which may result in overtopping of dam;
- Failure of upstream and downstream part of dam

- Liquefaction or loss of shear strength and its foundations due to pore pressure induced by the earthquake;
- Overtopping of dam due to large tectonic movement in the reservoir basin and waves due to due to earthquake induced landslides into reservoir from valley side;
- Damage of outlet work passing through the embankment

The potential for such damages depend on:

- Seismicity of the area
- Local and topographic conditions
- Type of dam
- Size of the embankment

The amount of site investigation, design and additional construction measures (over those needed for static conditions) will be depend on these factors and hazard rating of the dam (Fell, Macgregor and Stapledon, 1992)

Seed (1979) offered the possible defensive measures to overcome the potential harmful effects of the earthquakes on the embankment dams as follows:

- Using wide transition zones of material not vulnerable to carking

- Using chimney drains near the central potion of the embankment
- Allowing ample freeboard to allow for settlement, slumping or fault movements
- Using wide core zones of plastic materials not vulnerable to cracking
- Providing ample drainage zones to allow for possible flow of water through crakes
- Using well-graded filter zone upstream of the core to serve as crack stopper
- Flaring the embankment core at abutment contacts
- Stabilizing slopes around the reservoir rim to prevent slides into the reservoir
- Providing special details if there is danger of fault movement in the foundation
- Providing ample drainage zones to allow for possible flow of water through crakes

Considerable advances have achieved in analyzing stability of embankment dams during earthquake loading. Newmark (1965) introduced a method for predicting the permanent displacement of dams subjected to earthquake. Shear beam analysis method was used by Seed and Martin (1996) to study the dynamic response of embankment to seismic loads and presented a rational method for calculation. Later the finite element method was introduced to study the two-dimensional response of embankments (Idriss and Seed, 1967) and the equivalent linear method (Seed and Idriss, 1969) was used successfully to represent the strain-dependent nonlinear behavior of soils.

1.2. Aim of the Study

Dynamic behavior of Nahrain Dam, Tabas, Iran, under simulated earthquake motions was investigated. Simulated strong ground motions is assessed by considering the fault mechanism at the vicinity of the dam, provided by the Ministry of Electricity and water resources, Iran. Computer programs SAP 90, SAP 2000 and TELDYN are used during analyses. In this study dynamic response of the Nahrain Dam was investigated and permanent deformations were calculated.

Chapter II reviews the literature and the previous studies on the dynamic analysis and design of embankment dams and presents a summary of the computer programs used for the analyses. Chapter III provides a brief information about the seismicity of Iran and the Nahrain Dam region, its location and structure. Chapter IV presents the analysis procedure of Nahrain Dam and explains how dam modeled for static and dynamic analyses, how the material properties, input motion, yield acceleration are selected and used.

Results of the analysis are given in chapter V. Chapter VI is the conclusion chapter.

CHAPTER II

STATIC AND DYNAMIC ANALYSIS OF EMBANKMENT DAMS

2. 1. Static Analysis of Embankment Dams

Determination of static stress distribution in a dam is possible using approximate means (Lee and Idriss, 1975) and more accurate methods such as the finite element method. Finite element method can be used by performing the analysis in a number of steps, or increments. Non-linear incremental finite element analysis is used for approximating the nonlinear behavior of soil. In this procedure, the load is divided into a number of small increments, and the soil behavior is assumed to be linear elastic within each increment. In other words, the relationship between stress and strain is assumed to be governed by Hooke's law and this can be expressed as follows;

$$\begin{bmatrix} \Delta\sigma_X \\ \Delta\sigma_Y \\ \Delta\sigma_{XY} \end{bmatrix} = \frac{3K}{k-E} \begin{bmatrix} 3k+E & 3K-E & 0 \\ 3k-E & 3K+E & 0 \\ 0 & 0 & E \end{bmatrix} \begin{bmatrix} \Delta\varepsilon_X \\ \Delta\varepsilon_Y \\ \Delta\varepsilon_{XY} \end{bmatrix} \qquad (2.1)$$

where Δσ's are the stresses, K is the bulk modulus, E is the Young's modulus and Δε's are the strains.

The moduli for each element during each increment are evaluated in accordance with the stress in element and the iteration procedures is followed either until the compatibility between the assumed moduli and computed stresses is achieved or for a set number of iterations. (Pyke et al. 1984). Representation of changes in geometry during construction of the embankment, changes in loading of the reservoir and non-linear stress-strain behavior of the embankment materials are some of the advantages of incremental analysis in general and incremental finite element analysis in this case. FEDAM, ISBILD, LSBILD and TELSTA are such a finite element programs in which the method of construction of the dam is simulated by a progressive analysis where an additional layer of elements is added at each step. All these programs are designed for the plane strain condition. The programs consider the dependence of stress – strain behavior of the soil on the confining pressure and gives the initial tangent modulus, Ei, of the nonlinear stress strain curve as follows:

$$E_i = KP_a\left[\frac{\sigma_3}{Pa}\right]^n \qquad (2.2)$$

where σ_3 is the confining pressure, K is the modulus number,

n is an exponent determining the rate of change of Ei with σ_3 and

P_a is the atmospheric pressure in the same units as σ_3.

If a nonlinear analysis program is not available, a linear solution program such as SAP90 (Wilson and Habibullah, 1992) and SAP2000 non-linear version (Wilson and Habibullah, 2000) can be used to evaluate the state of stress throughout the body of the dam. In this case, since the program is a linear one, the initial solution will not be fully representative of the actual state of stress within the body of the dam. Since the stresses within an embankment are dependent on the elastic modulus of deformation, and also the elastic modulus of deformation is dependent on the state of the confining stress there may be some iterations necessary to calculate the actual values of elastic modulus and the state of the resulting stress. Baba (1982) has offered following equation in which the relation of elastic modulus of deformation, E, to the vertical stress, σ_y (kg/cm^2) is given:

$$E\ (\text{kg/cm}^2) = A\ \sigma^{B}_{y} \qquad (2.3)$$

Where A and B are constants for core, fill and filter portions of the dam.

2.2. Dynamic Analysis of Embankment Dams

Observation of the behavior of earth fill dams in the past earthquakes have highlighted the value of seismic stability evaluations in assessing the over all performance of an earth fill dam in a seismic area. The near failure of lower San Fernando Dam in February 9, 1971 San Fernando earthquake increased the importance such evaluations among design Engineers (Idriss, Duncan and Michael, 1998).

There are many dynamic analysis methods for dams, however only some of them such as pseudo-static analysis, shear-beam method and finite element method will be briefly mentioned in the following sections:

2.2.1 Pseudo _ Static Analysis Method

Use of pseudo-static method for the dynamic stability analysis of earth structures goes approximately 80 years back. In this approach effect of earthquake is represented by a horizontal and (or) vertical, accelerations.

Although much more accurate and comprehensive methods have been developed nowadays pseudo-static method still is a useful and simple method for the understanding the effect of earthquake on the dams and predicting approximately the stability situation of them.

In this method horizontal and vertical, inertial forces resulted from earthquake shaking is representing by F_h and F_v respectively. The magnitudes of these forces which are applied through centroid are equal to:

$$F_h = \frac{a_h \times W}{g} = K_h \times W \qquad (2.4)$$

$$Fv = \frac{a_v \times W}{g} = K_v \times W \qquad (2.5)$$

where a_h is horizontal pseudo-static, a_v is vertical pseudo-static acceleration, k_h is dimensionless horizontal pseudo-static coefficient, k_v is dimensionless vertical pseudo-static coefficient and W is the weight of the mass of soil block in consideration (Figure 2.1).

By employing moment equilibrium analyses safety factor is defined as:

$$FS = \frac{\mathrm{Re}\,sisting\ Moments}{Overturning\ Moments} = \frac{c \times L \times R}{E(W - K_v) + K_h \times F \times W} \qquad (2.6)$$

where c is shear strength R and L are radius and length of sliding circle respectively, F and E are moment arms.

Theoretically a value of FS = 1 would mean a slide but in reality a slope may remain stable in spite of FS being smaller than unity and it may fail at a value of FS>1, depending on the character of the slope – forming material (Seed, 1979). The most obvious example to this is the complete upstream failure of the Lower San Fernando Dam whose FS was found to be

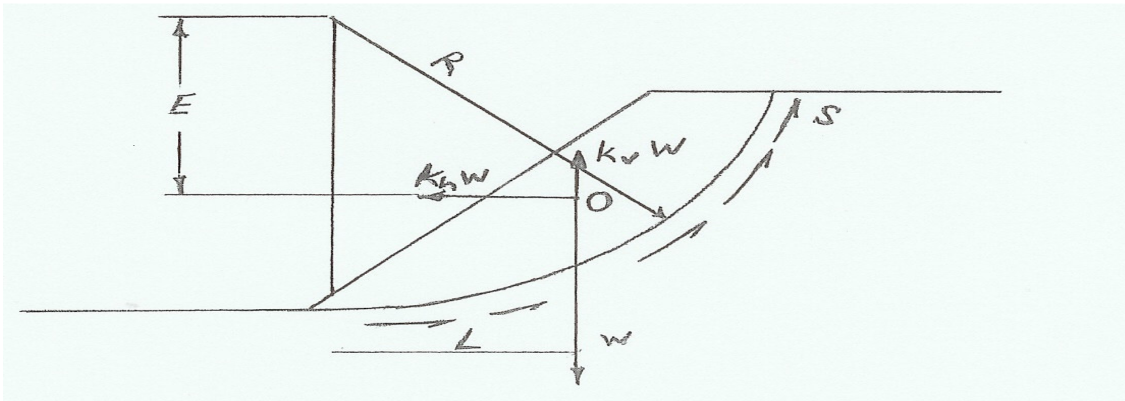

Figure 2.1 Magnitude of Forces Applied to Slip Surface.

1.3 using a seismic coefficient of 0.15, and movement of the crest of the Upper San Fernando Dam by 12 to 18 cm whose FS was calculated between 2 and 2.5. Another example is the failure of a Tailing Dam, Japan whose factor of safety was determined as approximately 1.3 and the seismic coefficient was selected to be 0.2 (Kramer, 1996). Therefore, it should always be noted that in designing an embankment dam by using the pseudo – static method, during the selection of the seismic coefficient, factors such as, type of the dam, geological conditions, type of the material used in construction, and the seismicity of the dam site should be considered.

As it can be seen from the above formula, the factor of safety has inverse proportionality to k_h, i.e. as the k_h increases, the factor of safety decreases.

Although it seems this method is simple and straightforward, the selection of k_h is very important and difficult. Not only k_h represents the earthquake characteristics but also reflects the material properties used for dam construction, geological conditions of the site etc.

Marcuson (1981) suggested that appropriate pseudo-static coefficient for dams should correspond to one-third to one-half of the maximum acceleration, including amplification and deamplification effects, to which dam is subjected.

2.2.2. Shear Beam Method

One of the earliest approaches to the dynamic analysis of two-dimensional geotechnical systems was the shear beam analysis applied to earth dams by Mononobe et al.(1936).This method has resulted in the reduction of computational cost and complexity of dynamic finite element analysis. This method typically involves simplifying a two-dimensional problem to a one-dimensional one. The shear beam approach is based on the following assumptions:

-A dam deforms in simple shear, thereby producing only horizontal displacements. Hatanaka (1952) and others have verified the accuracy of this assumption, at least for rigid foundation conditions.

-Either shear stresses or shear strains are uniform across horizontal planes. --

-Stresses and strains are nearly constant across the dam except in small zones near the upstream and downstream faces where they decrease to zero (Gazetas, 1987).

-Dam is homogeneous and infinitely long.

- Horizontal displacements are constant at a given depth.

-Influence of the reservoir is neglected.

Figure (2.2) shows basic model of this method.

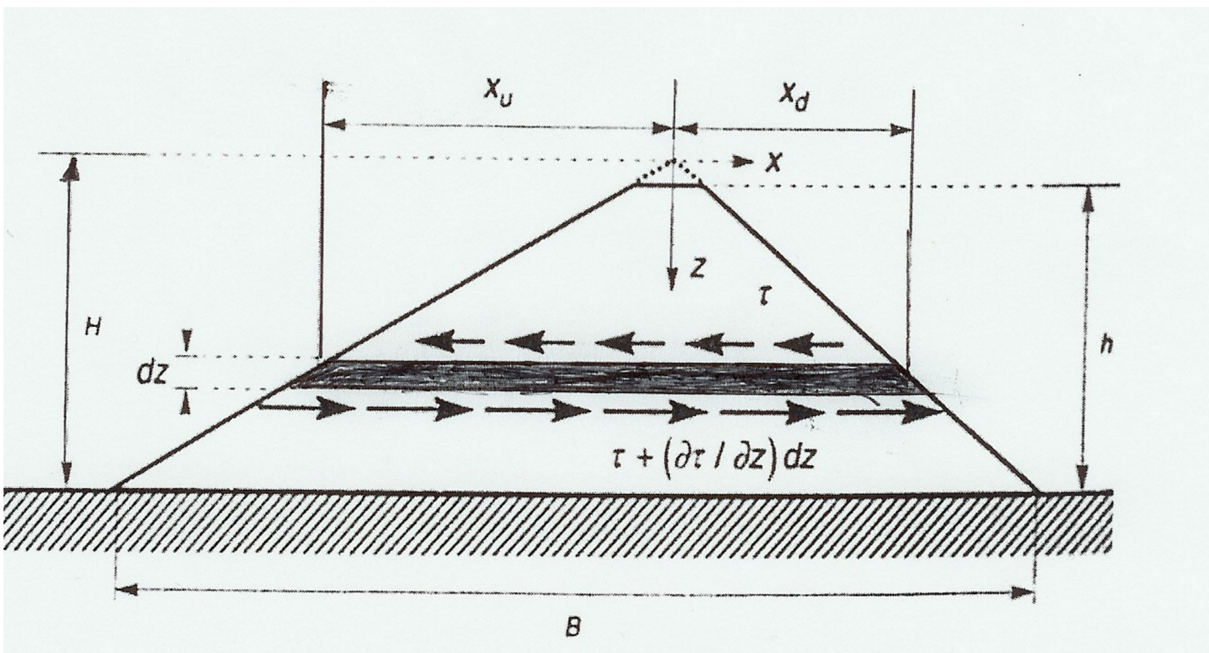

Figure 2.2. Earth dam showing stresses acting on an element of thickness dz (Kramer, 1996)

Assuming horizontal displacements to be constant at a given depth, the horizontal displacement relative to the base, u (z,t), is independent of x. The resultant shearing force on the upper surface of a slice of thickness, dz:

$$S_z(t) = \int_{-xd}^{xd} \tau(x,z,t)dx \tag{2.7}$$

The corresponding resultant shearing force on the bottom of the slice is:

$$S_{z+dz}(t) = \int_{-xd}^{xd} (\tau(x,z,t) + \frac{\partial \tau(x,z,t)}{\partial z} dz)dx \tag{2.8}$$

The resultant inertial force acting on the slice depends on the total acceleration is:

$$I_z(t) = \rho \left[\ddot{u}(x,z,t) + \ddot{u}_b(t)\right] \frac{2B\ z}{H} dz \tag{2.9}$$

For equilibrium in the x – direction,

$$S_{z+dz}(t) - S_z(t) = I_z(t) \tag{2.10}$$

Or

$$-\frac{\partial}{\partial z}\left[\int_{-xd}^{xd} \tau(x,z,t)dx\right] dz = \rho \left[\ddot{u}(z,t) + \ddot{u}_b(t)\right] \frac{2B}{H} dz \tag{2.11}$$

Substituting $\tau(x,z,t) = G(x,z)\gamma(z,t)\ and\ \gamma(z,t) = \partial u(z,t)$ the shear beam equation can be written as

$$\rho(\ddot{u}+\ddot{u}_b)=\frac{1}{z}\frac{\partial}{\partial z}\left[\overline{G}(z)z\frac{\partial u}{\partial z}\right] \tag{2.12}$$

Where the average shear modulus, $\overline{G}$ is given by:

$$\overline{G}(z)=\frac{1}{x_u+x_d}\int_{-xd}^{xd}G(x,z)dx \tag{2.13}$$

Gazetas (1987) developed solution to the shear beam wave equation for the case where the shear modulus increases as a power function according to $G(z)=G_h(z/h)^m$ where G_h is the average shear wave velocity of the soil at the base of the dam. For such condition, the n_{th} natural frequency (assuming h/H=1) is given by:

$$\omega_n=\frac{\overline{v}_{ss}}{H}\frac{\beta_n}{8}(4+m)(2-m) \tag{2.14}$$

where $\overline{v}_{ss}$ is the average shear wave velocity of the soil in dam, ω_n is the n-$_{th}$ mode of natural circular frequency and m is the stiffness parameter. β_n is the n-$_{th}$ root of a period relation. Values of β_n is generally tabulated for the first five modes of vibration of an earth dam.

Equation (2.14) produces a fundamental period of

$$T_1 = \frac{16\pi}{(4+m)(2-m)\beta_1} \times \frac{H}{\bar{v}_{ss}} \tag{2.15}$$

The mode shape at the nth natural frequency is given by

$$U_n(z) = \left(\frac{z}{H}\right)^{-m/2} J_q\left[\beta n\left(\frac{z}{H}\right)^{1-m/2}\right] \tag{2.16}$$

where J_q is a Bassel function. (Kramer et al 1996)

2.2.3. Finite Element Method.

The term “Finite Element “it is due to R.W.Clough (1960). The finite element method is actually an approximate technique for the numerical solution of differential equations that arise in engineering systems. The finite element method (FEM) involves the placing of suitable grid-work or mesh on the two-dimensional (generally) continuum and dividing it into triangular or rectangular elements connected at the nodes. (Wasti and Utku, 2001)

FEM is one of the most powerful methods in analyzing embankment dams under earthquake loading. In this method time dependent stress-strain behavior of each element and region can be determined. Irregular geometry and complex boundary conditions can be taken into account. In addition, nonlinearity of soil can be taken into consideration, since during seismic loading the materials, especially earth materials, is subjected to large shear deformations this condition introduced significant nonlinear behavior of the material.

The equation of motion for dynamic finite element method which represents the dynamic equilibrium of all elements can be written as:

$$[M]\{\ddot{u}\}+[C]\{\ddot{u}\}+[K]\{\ddot{u}\}=-\{m\}\ddot{y} \qquad (2.18)$$

where {u} is a vector containing the unknown motions relative to the rigid base and $\ddot{y}$ is the given time history of the base. The mass matrix [M], the damping matrix [C], and the stiffness matrix [K] can be assembled from the individual element matrices, and the matrix {m} is a vector related to [M]

Equation (2.17) can be solved by different numerical techniques such as:

-Modal Analysis.

-Fourier Analysis.

-Direct Integration.

The first two methods are suitable for linear elastic systems and the direct integration is the most common methods to evaluate non-linear behavior of the systems under cyclic loading.

Finite element methods are used for solution of two and three dimensional dynamic response analysis. In case of embankment dam three dimensional dam body is treated as two-dimensional because in transverse direction length of dam body is very long. Therefore, dam is assumed to behave according to plane strain conditions. There are many computer programs, which analyses the dynamic behavior of dam using plane-strain assumption. QUAD-4 (Idriss et al 1973), LUSH (Lysmer et al. 1974) FLUSH (Lysmer et al. 1975) and TELDYN (Pyke et al 1984). The last one, which is employed in the present analysis, is a computer program designed for equivalent linear, plane strain, and dynamic finite analysis of soils.

2.2.3.1. Equivalent Linear Model

The concept of equivalent - linear seismic analysis involves conduct of several iterations in order to obtain shear modulus and damping ratio in each element that are compatible with the average level of shear strain induced by shaking. This equivalency consists of two steps:

1) Within each cycle of loading the shear stress-shear strain relationships for soils are non-linear and exhibit hysteretic damping as shown in figure (2.3). As the cyclic shear strain amplitude increases, the average modulus decreases and hysteretic damping, as indicated by the enclosed stress-strain curves, increases. As shown in figure (2.3) the average or “equivalent linear” shear modulus can be represented by the secant modulus drawn through the ends of hysteretic loops. The hysteretic damping can be

converted into an "equivalent viscous damping ratio" using the following formula:

$$\lambda = \frac{\Delta W}{4\pi \times W} = \frac{A_L}{4\pi A_H} \tag{2.19}$$

where ΔW is dissipated energy represented by the hysteretic loop, W is the maximum energy represented by the hatched area, A_L and A_H are area of the hysteretic loop and area of the hatched section respectively.

It should be noted this conversion actually requires that the hysteretic loops be presented by ellipses. At small strains, the approximation involved is not too bad however, at larger strains, the approximation becomes very crude, especially when shape of the hysteretic loops degenerates as is common for many soils. Nonetheless, if equivalent linear shear modulus and the equivalent viscous damping ratio are measured in laboratory tests, which can cover a wide range of shear strains, curves showing the reduction of the modulus and the increase in the damping ratio with increasing cyclic shear strain can be obtained, as shown in figures (2.4) and (2.5)

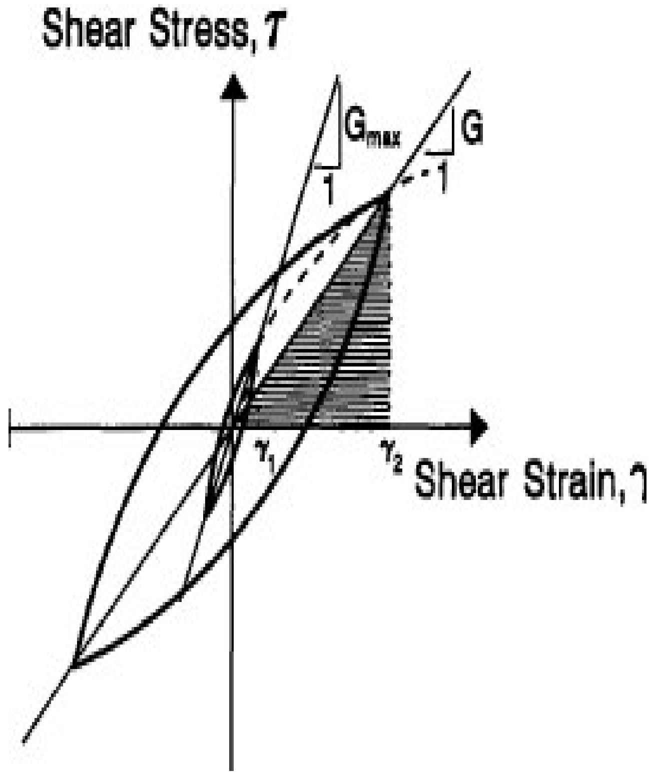

Figure 2.3 Hysteretic stress-strain relationship at different strain amplitudes (Rowlins et al. 1998).

2) The second step in the equivalency process involves choosing an appropriate average shear strain to use in determination of the modulus and damping values to be used in the analysis.

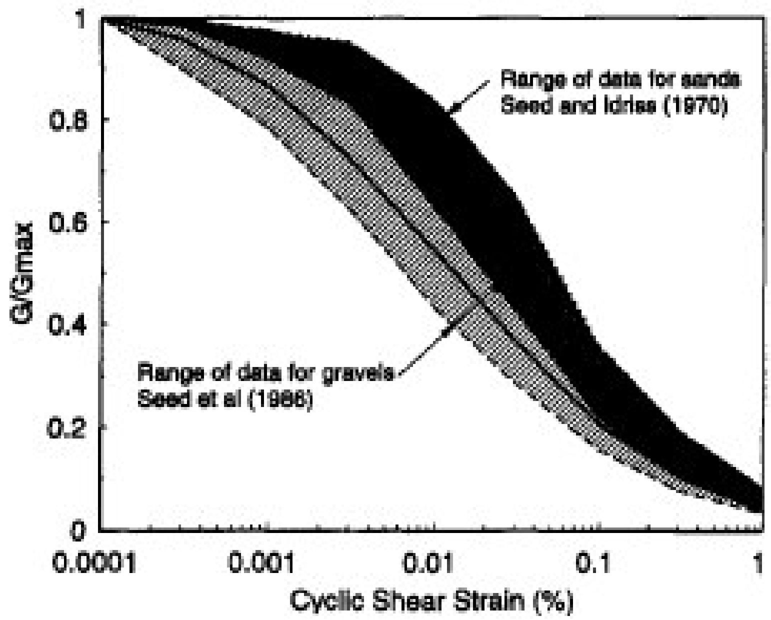

Figure 2.4 Typical shear modulus reduction curve, G/G_{max} versus γ relationships for sands (Seed and Idriss 1970) and gravels (Seed et al. 1986)

G_{max} can be computed from the following formula:

$$G_{\max} = \rho \; V_s^{\,2} \qquad (2.20)$$

where ρ is mass density of the soil and the V_S is the shear wave velocity, which can be measured either by seismic field test or in laboratory at low stains.

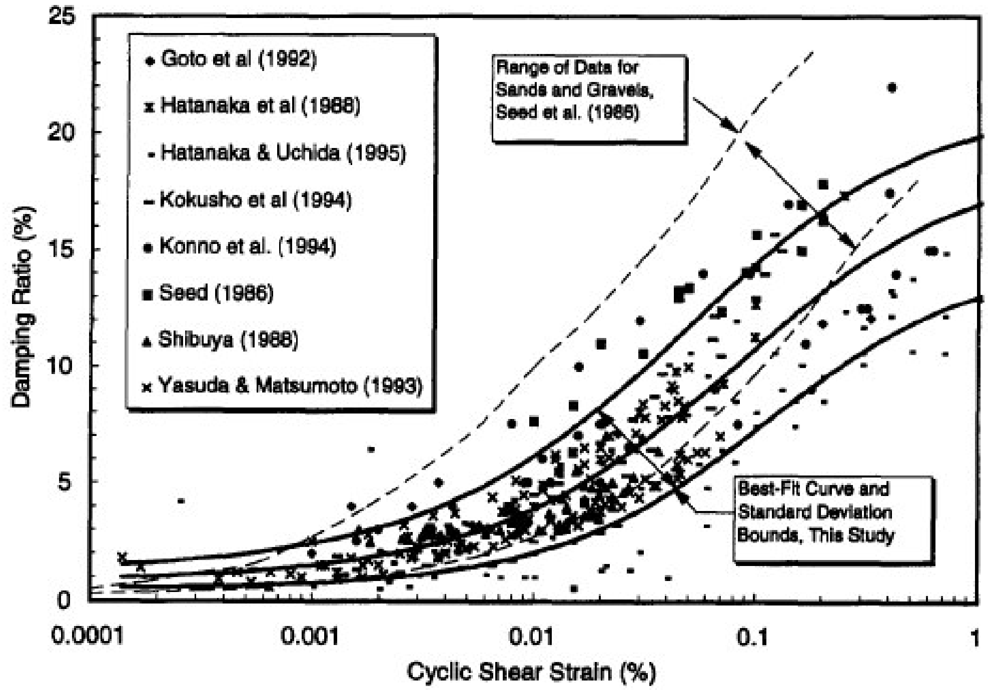

Figure 2.5 Typical damping ratio curves from eight investigations for gravelly soils (Seed et al. 1986)

G_{max} can also be estimated by SPT and CPT. Following formula can also be used for the estimation of the G_{max} :

$$G_{max} = 1000\ k_{2,max}\ (\sigma'_m) \qquad (2.21)$$

here $K_{2,\,max}$ is coefficient varying from 30 - 80 for clean sands and 80-180 for gravelly soils, σ'_m is the mean effective stress in psi (Seed et al. 1984).

2.3. Permanent Displacement Analysis.

For the first time Newmark introduced the permanent displacement method in 1965. He has introduced this method as an alternative to pseudo-static method. Pseudo-static method, like all limit equilibrium methods give no idea about plastic deformation. Since earthquake-induced accelerations vary with time, the pseudo static factor of safety will vary throughout an earthquake. If the inertial forces acting on a potential failure mass become large enough that the total (static plus dynamic) driving forces exceed available resisting forces, the factor of safety will drop below 1.0. Newmark's method evaluates such a condition. When the factor of safety drops below 1.0, the potential failure is no longer in equilibrium; consequently, it will be accelerated by unbalanced forces. (Kramer, 1996)

The calculation is based on the assumption that the whole sliding mass moves as single rigid body with resistance mobilized along the sliding surface. The situation is analogous to a block resting on an inclined plane (figure 2.6).

Consider the block in stable, static equilibrium on the inclined plane of figure 2.6b. Under static conditions, equilibrium of the block (in the direction parallel to the plane) requires that the available static resisting force, *Rs,* exceed the static driving force, *Ds* (Figure 2.8a). Assuming that the block's resistance to sliding is purely frictional (c = O)

$$FS = \frac{available\ resisting\ force}{static\ driving\ force} = \frac{Rs}{Ds} = \frac{W\ \cos\beta\ \tan\phi}{W\ \sin\beta} = \frac{\tan\phi}{\tan\beta} \qquad (2.22)$$

where Φ is the angle of friction between the block and the plane and β is the angle between the slope and horizontal x-axis. Now consider the inertial forces transmitted to the block by horizontal vibration of inclined plane with acceleration, $a_h(t) = k_h(t)g$, (a_y is neglected for simplicity). At a particular instant of time, horizontal acceleration of the block will induce a horizontal inertial force, k_hW (figure 2.8 b) when the inertial force acts in the down slope direction, resolving forces perpendicular to the inclined plane gives:

$$FS = \frac{available\ \ resisting\ \ force}{pseudo-static\ \ driving\ \ force} = \frac{R_d(t)}{D_d(t)} = \frac{[\cos\beta - k_h(t)\sin\beta]\tan\phi}{\sin\beta + k_h(t)\cos\beta} \qquad (2.23)$$

The dynamic factor of safety decreases as k_h increases and some positive value of k_h which produce a factor of safety of 1 is called *yield coefficient,* k_y which corresponds to *yield acceleration,* $a_y=k_yg$. The yield acceleration is the minimum pseudo static acceleration required to produce instability of the block. (Kramer, 1996)

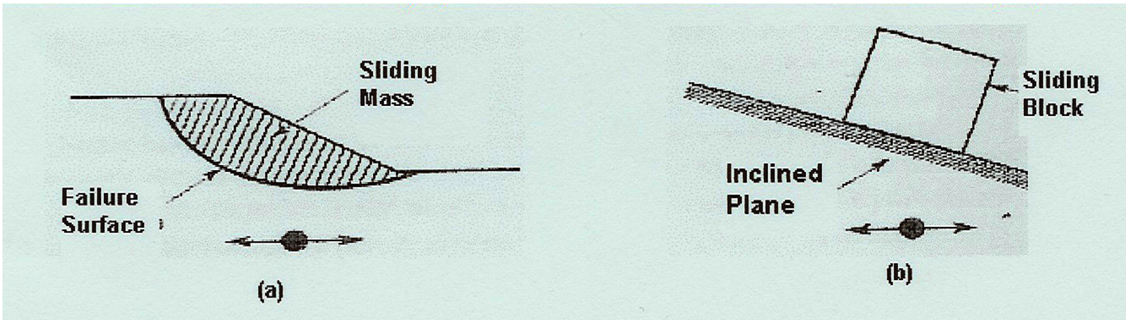

Figure 2.6. Analogy between (a) potential landslide and (b) block resting on inclined plane. (Kramer, 1996)

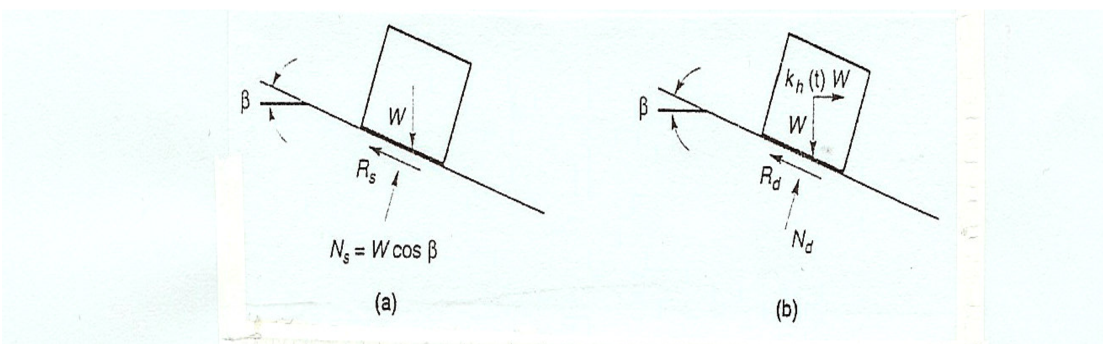

Figure 2.7 Forces acting on a block resting on an inclined plane: (a) static conditions: (b) dynamic conditions. (Kramer, 1996)

Considering the slope and sliding block analogy the block on the inclined plane subjected to pulse acceleration greater than the yield acceleration, the block will move relative to the plane. Relative acceleration of the block regarding to plane is:

$$a_{rel} = a_b(t) - ay = A - ay \qquad t_0 \leq t \leq t_0 + \Delta t \qquad (2.24)$$

where $a_b(t)$ is the acceleration of the inclined plane. The relative movement of the block during this period can be obtained by integrating the relative acceleration twice, that is:

$$V_{rel}(t) = \int_{t_0}^{t} a_{rel}(t)dt = \left[A - a_y\right](t - t_0) \qquad t_0 \leq t \leq t_0 + \Delta t \qquad (2.25)$$

$$d_{rel}(t) = \int_{t_0}^{t} vrel(t)dt = \frac{1}{2}\left[A - ay\right](t - t_0)^2 \qquad t_0 \leq t \leq t_0 + \Delta t \qquad (2.26)$$

Following procedure is used to calculate the actual displacement of the sliding slope. The average time history of acceleration of the sliding mass can be taken as the acceleration time history, *$a_b(t)$*. To determine *$a_b(t)$* firstly sliding mass should be divided into strips or finite elements. Secondly, the average time history of each slice or elements $a_{ib}(t)$ should be determined from the dynamic finite element analysis. At next stage, each force time history is obtained by multiplying the acceleration of each element with its mass, m_{ib} . Total force on an individual strip or element is calculated as follows;

$$F_b(t) = \sum F_i(t) = \sum m_{ib} \times a_{ib} \tag{2.27}$$

Finally, the average time history of sliding mass is calculated by dividing total force by total mass of sliding slope.

$$a_b(t) = \frac{Fb(t)}{mb} = \frac{\sum m_{ib} \times a_{ib}(t)}{\sum m_{ib}} \tag{2.28}$$

And, by integrating twice of average function $a_b(t)$, permanent displacement of the slope is determined. (Figure 2.8)

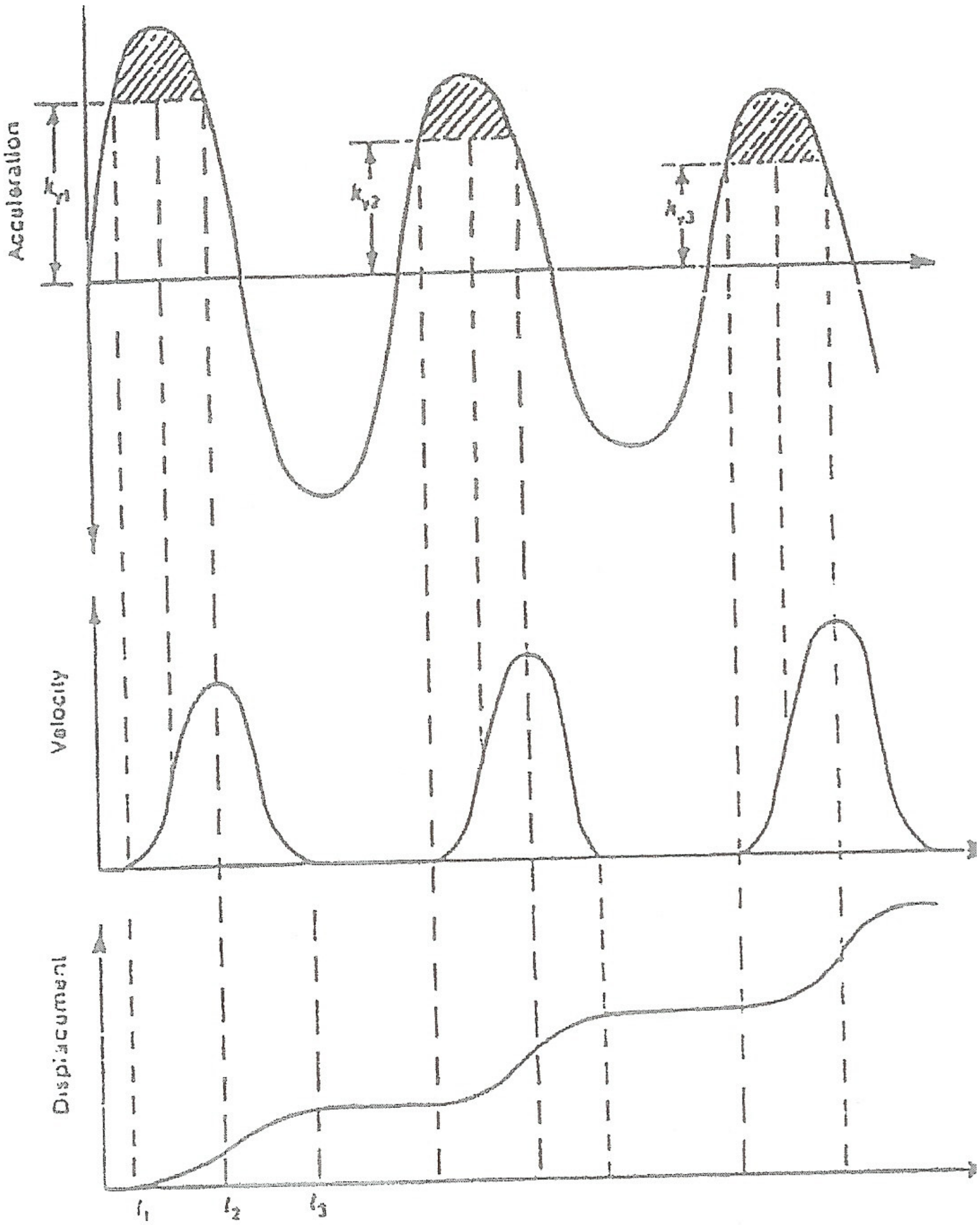

Figure 2.8 Integration of Effective Acceleration Time – History to Determine Velocities and Displacements (After Seed, 1979)

CHAPTER III

GEOLOGICAL & DESIGN INFORMATION OF NAHRAIN DAM

3.1 FAULT MECHANISM OF CENTRAL AND EASTERN IRAN

The active deformation of Iran is controlled by Arabian-Eurasian convergence. Shortening is mainly accommodated by distributed faulting in high mountains of the Zagros (Z) in the south, and the Alborz (A) and Kopeh Dagh (K) in the north (Figure 3.1).

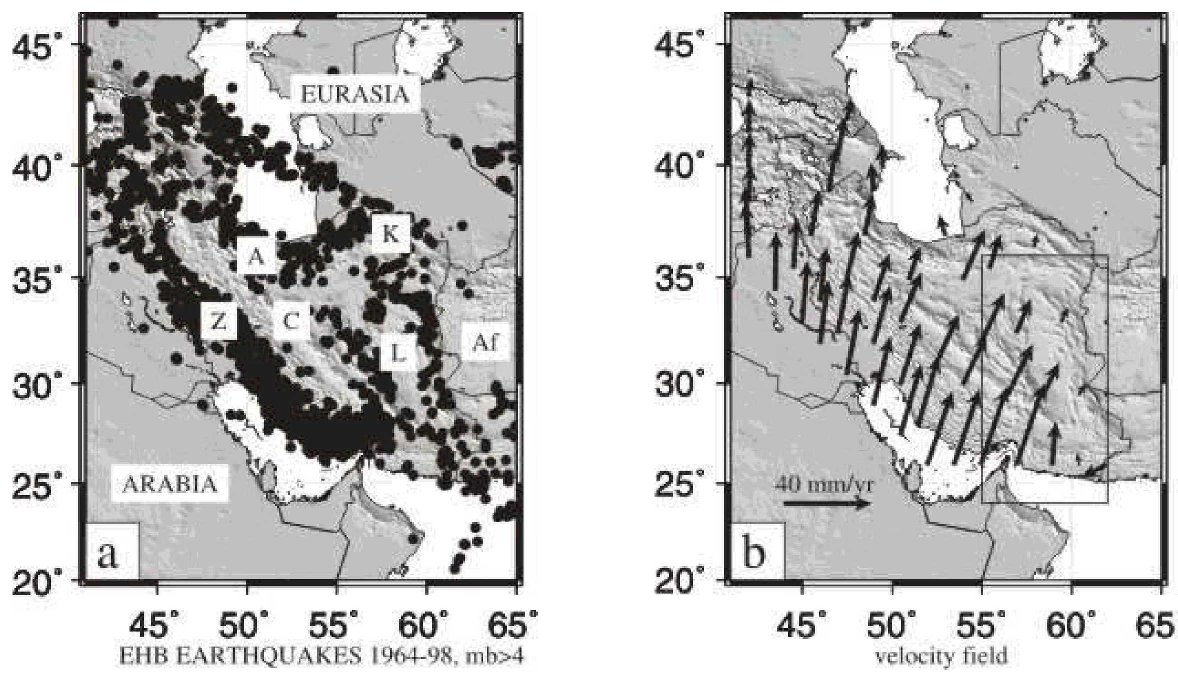

(a) ***(b)***

Figure 3.1.(a) Seismicity of Iran 1964-1998 (from the catalogue of Engdahl et al, 1998). (b) A velocity field for Iran estimated from variation in strain rates indicated by earthquakes (Walker, 1995).

Arabian-Eurasia convergence is about 26 to 30 mm/yr at the longitude of eastern Iran. It seems likely that about half of this is taken up in the Zagros, leaving about 15 mm/yr to be accommodated in the Alborz and central Iran. This must be the cause the same amount of right-lateral shear in eastern Iran. There are several indications that the present-day tectonic configuration dates from around 5 million years ago. We therefore have some idea of how much deformation must be accounted for on the active faults.

Central Iran is one of the main units of Iran, which is triangular in shape. It is one of the biggest and the most complicated unit of Iran. It also can be counted as the oldest plate of Iran. Its eastern boundary is not well known. Eastern Iran is a region of widespread active faulting (Figure 3.2) and many of these fault systems have been responsible for destructive earthquakes, and pose a serious seismic hazard to local populations. However, little is known of their evolution, development, and rate of slip.

Right-lateral shear is taken up on several north-south right-lateral fault systems that surround the Lut desert (aseismic block that is probably not deforming). In the north, the right-lateral shear is seen as clockwise rotation about vertical axes of east-west left-lateral faults (the Doruneh and

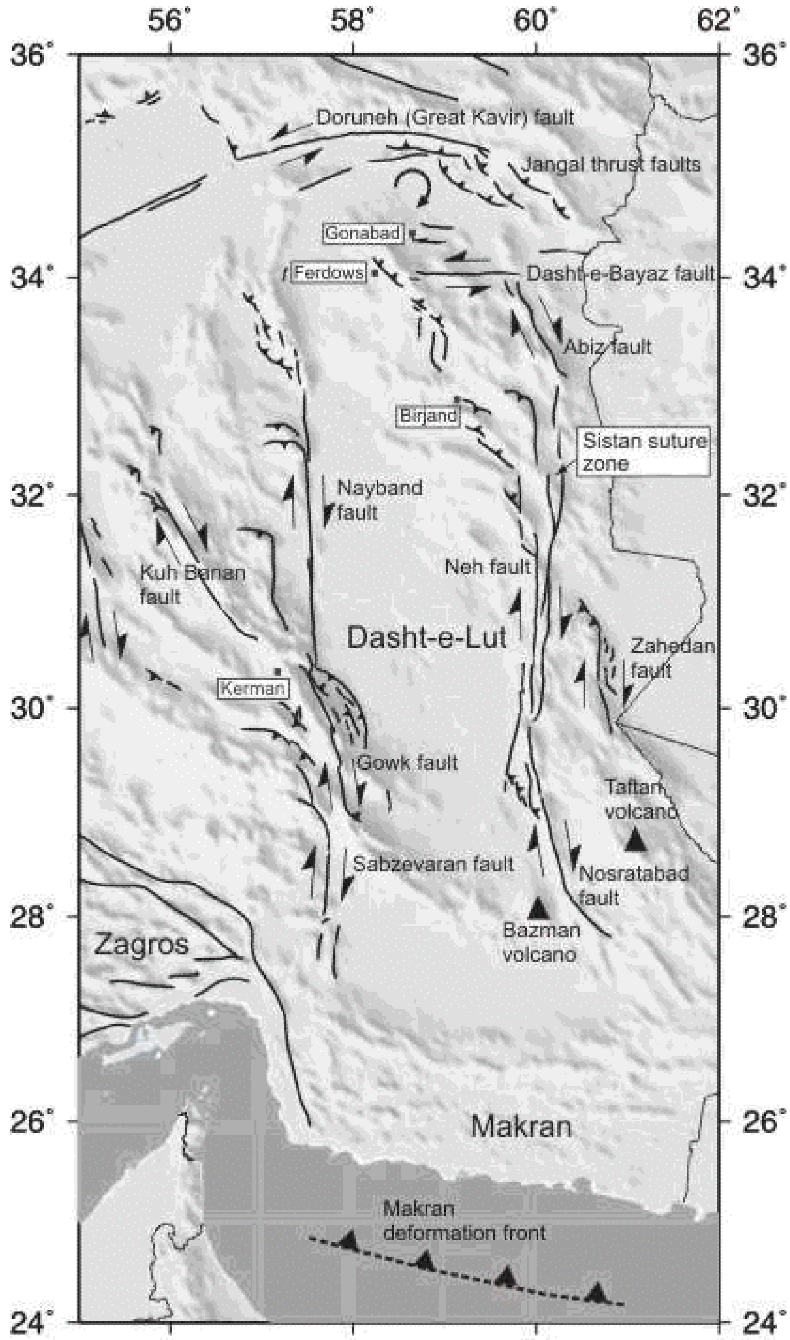

Figure 3.2. Fault map of eastern Iran. (Walker, 1995).

Dasht-e-Bayaz faults). Shortening components associated with the strike-slip faults result in widespread thrust faulting. These thrust faults often fail to reach the surface (termed 'blind' faults).

3.1.1. Thrust Faulting in Eastern Iran

Previously unrecognized thrust faults in eastern Iran were responsible for a destructive earthquake at Tabas (16 September 1978), which produced over 80 km of distributed and discontinuous surface ruptures above a series of low anticlinal hills to the west of a major range-front. Analysis of long-period body-wave seismograms shows a simple rupture on a gently dipping (~16 degrees) thrust, with a slight right-lateral component. Tabas Fault with N-S alignment is the nearest and the most active fault to the Nahrain dam. The mechanism is shown in figure (3.3)

3.2. Location of Nahrain Dam and Region Geology

Nahrain dam is located in Shotori Mountains in Tabas Block. It has been constructed on the Nahrain river (Sar dar river) and located between 33º 35´ to 33º 40´ latitude and 57º 05´ to 57º 10´ longitude (figures 3.4 and 3.5). The river width at the base of the dam is 63m and at the height of 45m from the base it is 170m. In other words, the width of the valley is 63 meters in the riverbed and 170 meters near the crown of the dam. Elevation of dam

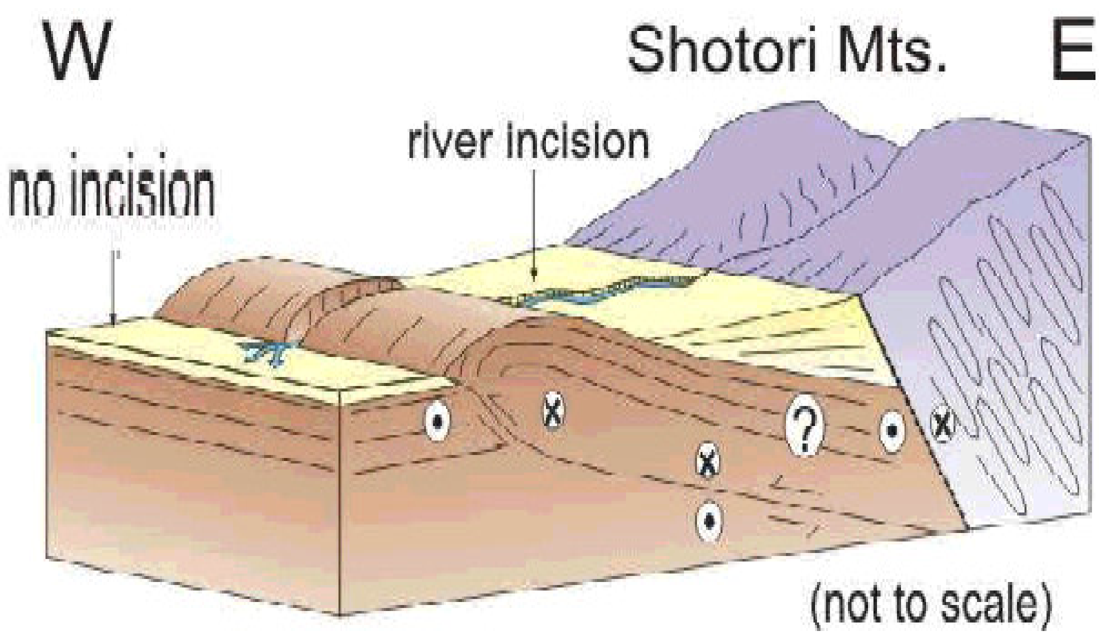

Figure 3.3 Schematic cross-section through the Tabas thrust fault (Walker, 1995)

Location is 1160m from mean sea level. Slope of the river at the dam location is approximately 2.0%. Geotechnical investigation shows that depth of the river deposits (wash) and weathered shale is 6m each along the dam axis. During construction of the dam, these layers are removed and clay core is rest on the shale. Left abutment is composed of shale and sandstone, which has 32 º slopes. Right abutment is approximately normal to river surface and normal condition is stable enough. However, for construction of the dam, its slope was grouted and stabilized. Schematic view of the Nahrain dam is shown in figure 3.6. Material properties used for the construction of dam is shown in table 3.1.

Figure (3.4) is Landsat image of Tabas region. There are many faults in the dam region which their general specification are listed in table 3.2

As previously stated the most active and youngest fault of region is Tabas fault. One of the recent activation of this fault was realized during in 1978 earthquake. This fault is 55 km long and possible rapture is predicted to be about 36 km. Using Mohajer and Norouzi method (1978) an earthquake with a 6.9 in Richter magnitude is predicted. Using Hosner(1969), Saymonz(1977), Toucher(1978), and Peres(1967) method magnitude of probable earthquake for this fault and the other faults of the region regarding their rupture length are determined and summarized in table 3.3.

Table 3.1 Material used for Construction of Nahrain dam (NDAR, 1994)

Layer No.	Layer Name	Coefficient of Friction Angle	Cohesion, c t/m2	Unit Weight γ (t/m3)
1	Skin	38	0	2.2
2	Skin	37.5	0	2.2
3	Skin	37	0	2.2
4	Filter	35	0	2.2
5	Clay Core	29	2.0	2.0
6	Clay Core	28.5	2.0	2.0
7	Clay Core	28	2.0	2.0
8	Rock Toe	40	0	2.4
9	Wash	34	0	2.2
10	Weathered Shale	30	1.0	2.5
11	Shale	32	1.5	2.5

Table 3.2 Major Fault Specifications within 100 km from Nahrain Dam (NDAR, 1994)

No.	Fault Name	Alignment	Length of fault (km)	Distance from Nahrain Dam(km)
1	Chashmeh Rostam	E-W	135	63
2	Golmorad	NNE-SSW	250	65
3	Nayband	N-S	400	20
4	Nayini	NNE-SSW	32	82
5	Spak	NNW-SSW	77	5
6	Tabas	N-S	55	13

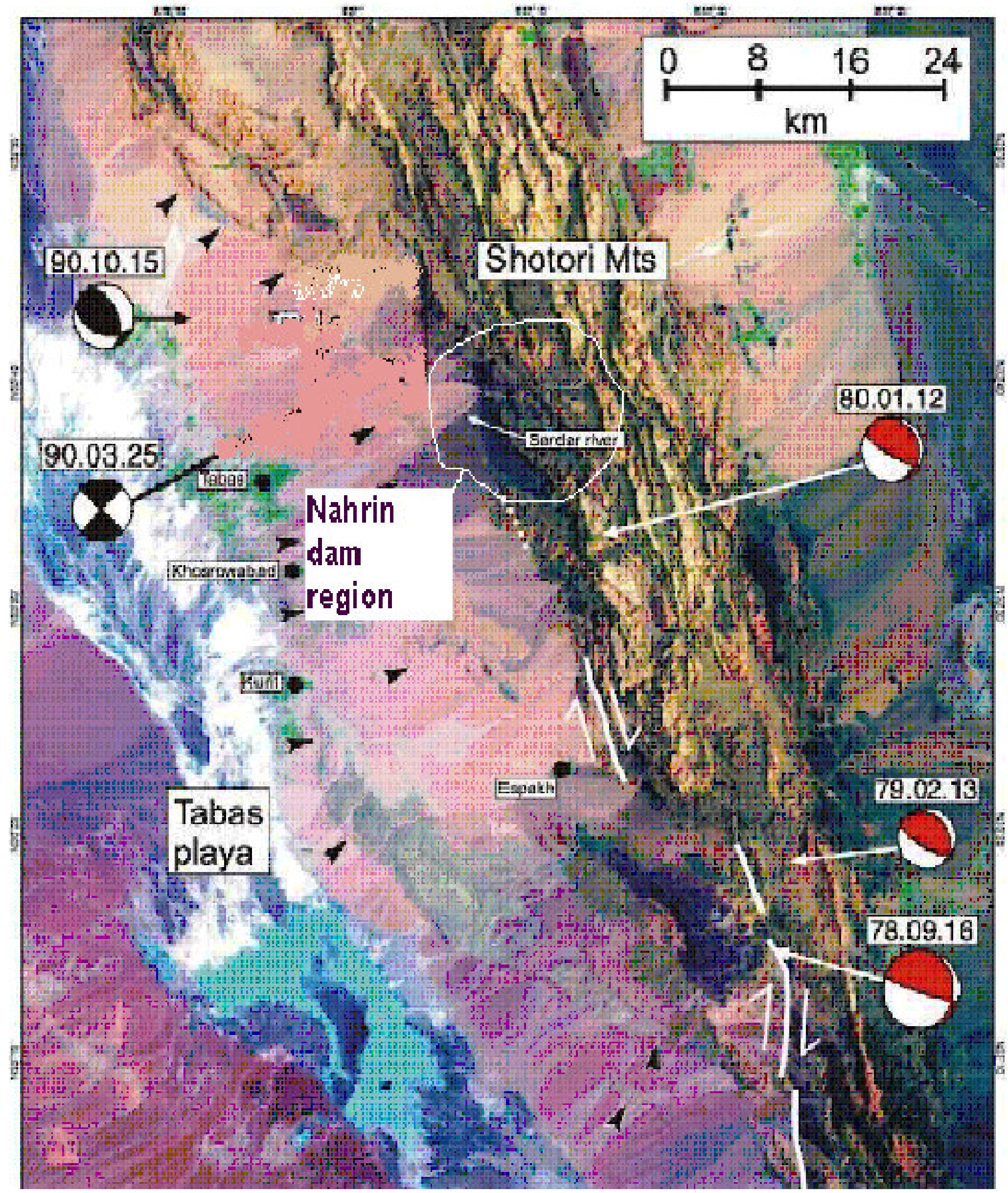

Figure 3.4 Land sat image of the Tabas region (Walker, 1995).

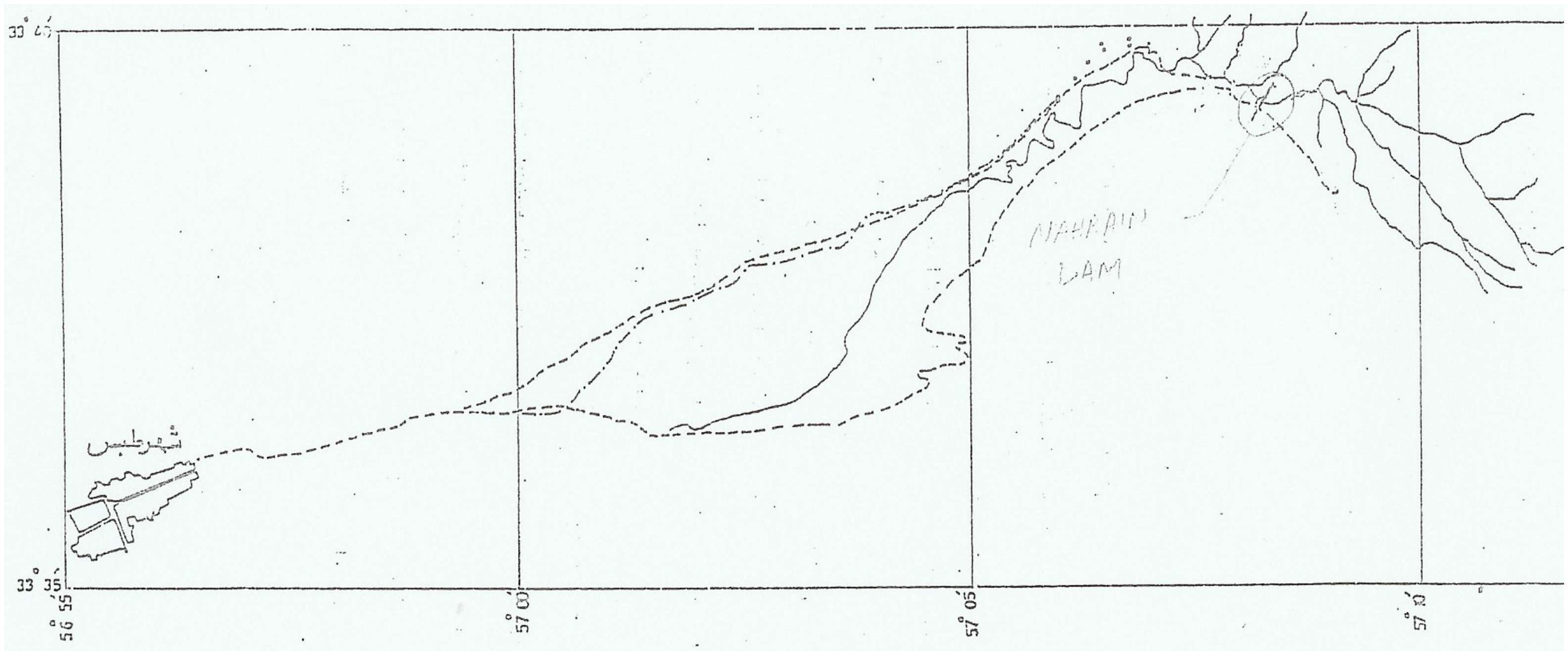

Figure 3.5 Location of Nahrain Dam

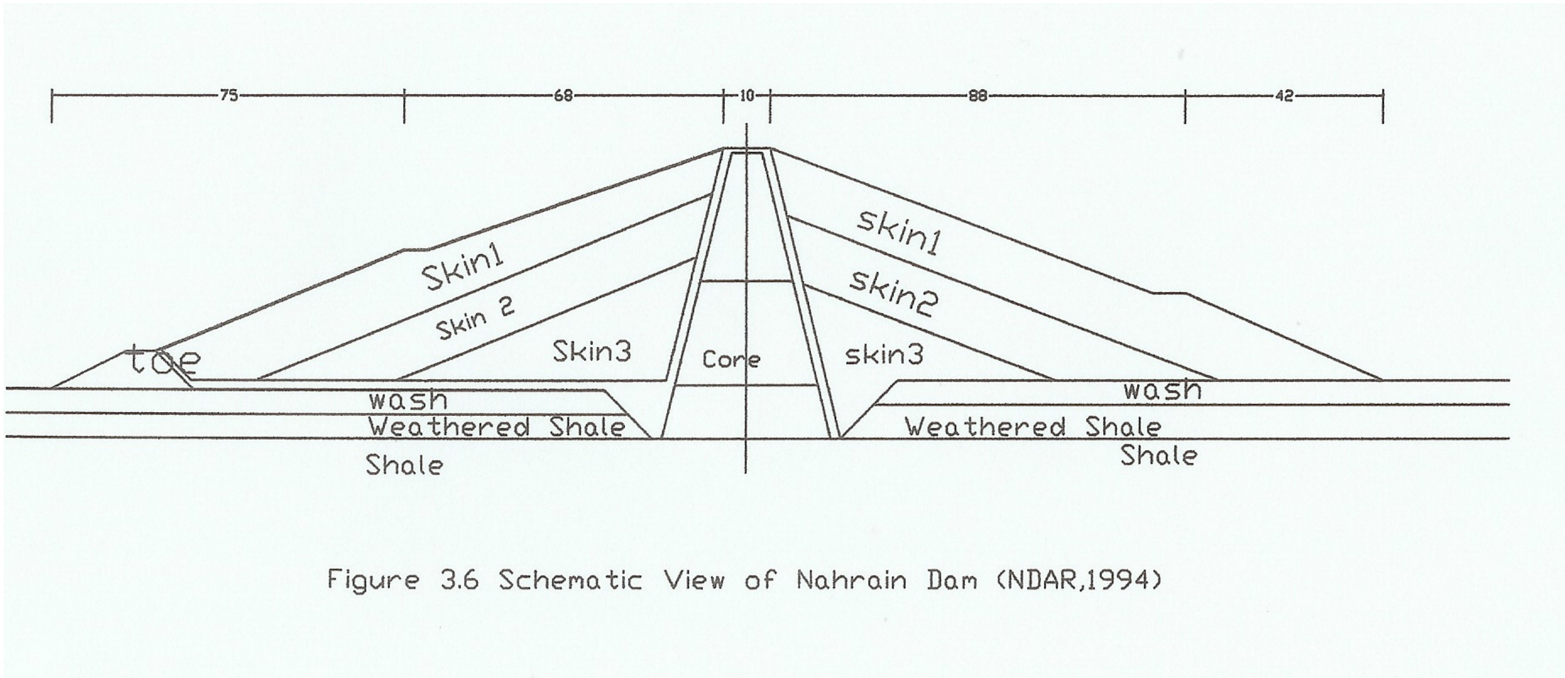

Figure 3.6 Schematic view of the Nahrain dam

3.3. Probabilistic Assessment

In this study, an area with 300 km radius was selected. Magnitude of past earthquakes is taken into consideration. Also probable earthquakes considering different risk, corresponding to the different lifetime of the dam was calculated. Gamble type III distribution function (3.1) is used to calculate the probable earthquake magnitude(NDAR, 1994).

$$P(M) = \exp(-C \bullet \exp\{\, B \bullet \ln[M_{\max} - Mi]\ \} \qquad (3.1)$$

where P (M) is the improbability of occurring and earthquake greater than magnitude M, M_i is the maximum measured magnitudes during five year periods and C & B are coefficients depending on the dimension of the region and the number of years. Using the largest earthquake during year 1903 until 1989 within 300 kilometer radius from the dam the parameters B and C are found as(appendix-A). B =1.7869 And C =0.0389. Summary of this calculation is shown in table 3.4.

Table 3.3 Different earthquake estimation methods with respect to the length of predicted rupture (NDAR, 1994)

Fault Name	Fault Length (km)	Probable Rupture Length (km)	Predicted magnitude of probable earthquakes by different methods					Average	Standard Deviation
			Hosner	Mohajer & Norouzi	Peres	Touchier	Symons		
Chashmeh Rostam	135	68	8,0	7,2	7,6	7,5	7,1	7,5	0,31
Golmorad	250	125	8.4	7.5	7,9	7,8	7,4	7,8	0,33
Nayband	400	200	8,7	7,7	8,1	8,0	7,7	8,0	0,36
Nayini	32	16	7,1	6,6	7	6,9	6,5	6,8	0,23
Spak	77	38	7,7	6,9	7,4	7,2	6,9	7,2	0,30
Tabas	55	36	7,7	6,9	7,4	7,1	6,9	7,2	0,31

Table 3.4 Magnitude of probable earthquake considering different risks for different

lifetimes of the dam

Life time of the dam (years)	Risk percentage	Return Period (years)	Earthquake Magnitude (MS)
35	64 37 10	25 55 238	6.9 7.3 7.7
50	67 37 10	50 110 475	7.3 7.5 7.8
100	64 37 10	98 217 950	7.5 7.7 7.9

Using McGouwar empirical relation and Gamble type III distribution function considering above mentioned conditions, peak ground accelerations at dam site were determined by:

$$PGA = \exp(-C \bullet \exp\{B \bullet \ln\left[A_{\max} - A_i\right]\} \qquad (4.2)$$

Summary of this calculation is shown in table 3.5

Table 3.5 Peak Ground Acceleration considering different risks for the different lifetimes of the dam (NDAR, 1994)

Life time of the dam (years)	Risk percentage	Return Period (years)	peak ground acceleration (cm/s^2)
25	64 37 10	25 55 238	120 180 320
50	67 37 10	50 110 475	175 260 390
100	64 37 10	98 217 950	250 310 420

Table 3.6 shows summary of the data used for this analysis.

Table 3.6 Summaries of the Data (NDAR, 1994)

Earthquake	Risk (%)	Magnitude (Ms)	PGA (cm/s^2)
Normal Earthquake	64	7.3	175
Design Earthquake	37	7.5	260
Maximum probable Earth quake	10	7.8	390

Chapter IV

ANALYSES OF NAHRAIN DAM

4.1 The Analysis Procedure Utilized for Nahrain Dam

Design of Nahrain Dam was completed in 1996 by Ministry of Electricity and Water Resources. Pseudo – static method was employed for earthquake design and the seismic coefficient was selected as 0.26 g as in the most of the dams located in seismically active zones. With the increasing capacity of computers and other tools, finite element method is now much more preferred for dam analysis: therefore Nahrain Dam is reevaluated by means of finite element method. Two different finite element programs are used to evaluate the response of the dam. The following procedure is applied step-by-step in both programs.

1. The most critical surface of the dam was determined by using the computer program SLOPE in order to obtain corresponding yield acceleration, a_y.

2. Static analyses of the dam were performed with the finite element programs SAP90 and SAP2000 (Nonlinear) in order to find the effective confining pressures of the finite elements of dam body.

3. The dynamic material properties of Nahrain Dam were determined by using the effective confining pressures used for estimating maximum shear modulus.

4. The dynamic analyses of Nahrain Dam were performed by using the mentioned 2 different input motions in the finite element program TELDYN. The program uses equivalent linear method and plain strain condition.

5. The acceleration time history of the sliding block was calculated by using the acceleration histories of the required points, obtained from the dynamic analysis.

6. The permanent displacement for the whole sliding mass was computed by using the acceleration time history of the sliding block, according to Newmark's method.

4.2. Pseudo-static analyses of Nahrain Dam

For the pseudo static analyses of the Nahrain Dam program Slope-7 (Borin 1983) is used. Earthquake forces can be modeled in a pseudo static manner by specifying horizontal and vertical acceleration factors. As mentioned in the previous sections horizontal acceleration factor is the most effective factor in the pseudo static analysis. In this study, the vertical acceleration is not considered.

The pseudo static analysis is applied to determine critical slip surface. About 300 trial circles for each side of the dam were drawn. Factor of safety of each circle was determined and the minimum factor of safety for each set of trails was selected. After determination of critical slip surface the yield acceleration was determined for this surface. In other words a yield acceleration was found that makes the factor of safety of critical slip unity.

Yield acceleration was determined to both downstream and upstream slopes of the dam for the full reservoir case. Trial surfaces and results of this analysis are summarized in tables 4.1 and 4.2. Some of trial circles are shown in figures 4.1 to 4.10.

Table 4.1 Static Factor of Safety for Different Trial Slip Surfaces of Downstream and Upstream faces.

	Downstream	**Upstream**
Trial slip circle	Static safety factor	Static safety factor
1	2,503	2.215
2	2.299	2.307
3	3.102	2.337
4	2,88	2.384
5	3.15	2.506
6	3.05	2.720

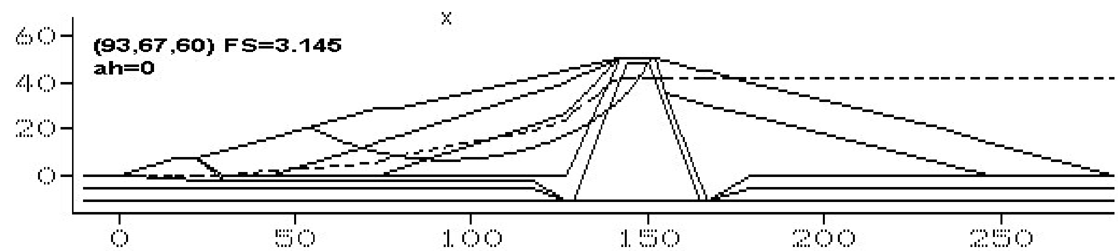

Figure 4.1 Trial circle no. 5 for Downstream Face

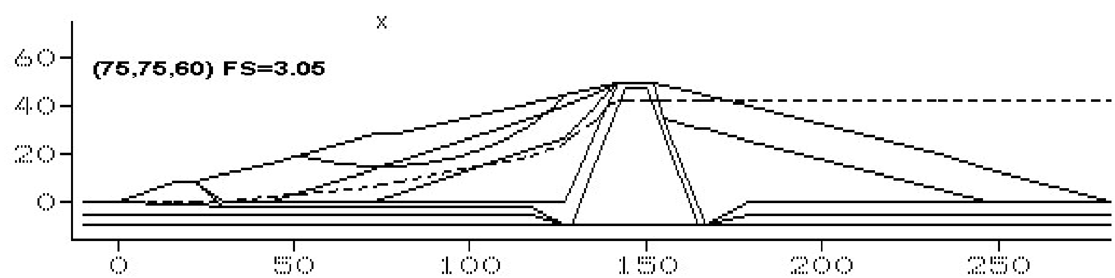

Figure 4.2 Trial circle no. 6 for Downstream Face

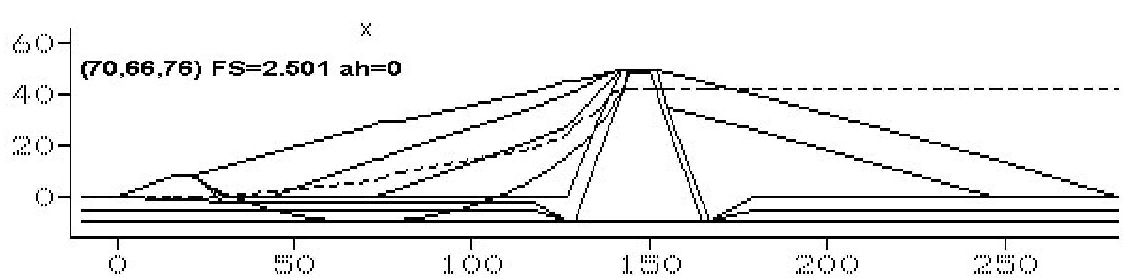

Figure 4.3 Trial circle no. 1 for Downstream Face

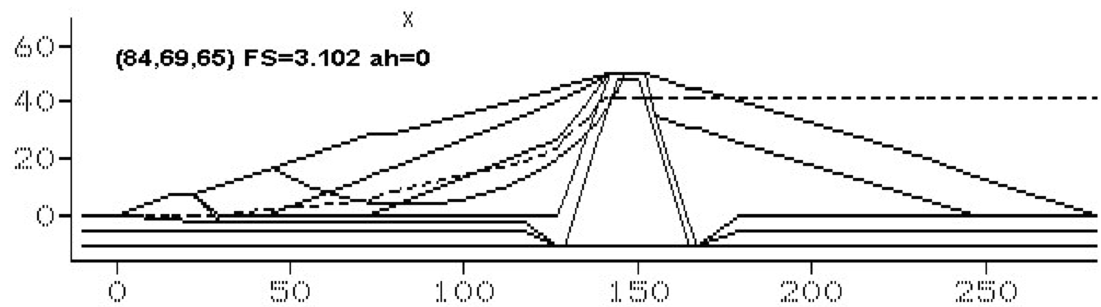

Figure 4.4 Trial circle no. 3 for Downstream Face

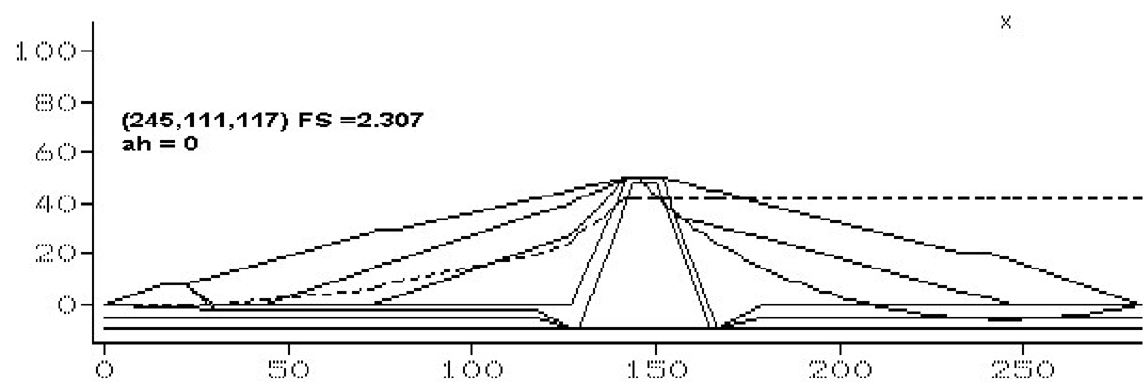

Figure 4.5 Trial circle no. 2 for Upstream Face

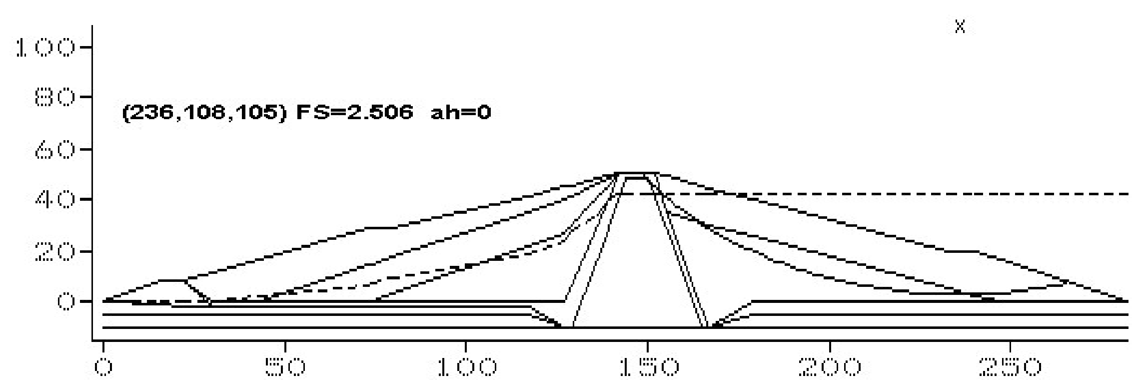

Figure 4.6 Trial circle no. 5 for Upstream Face

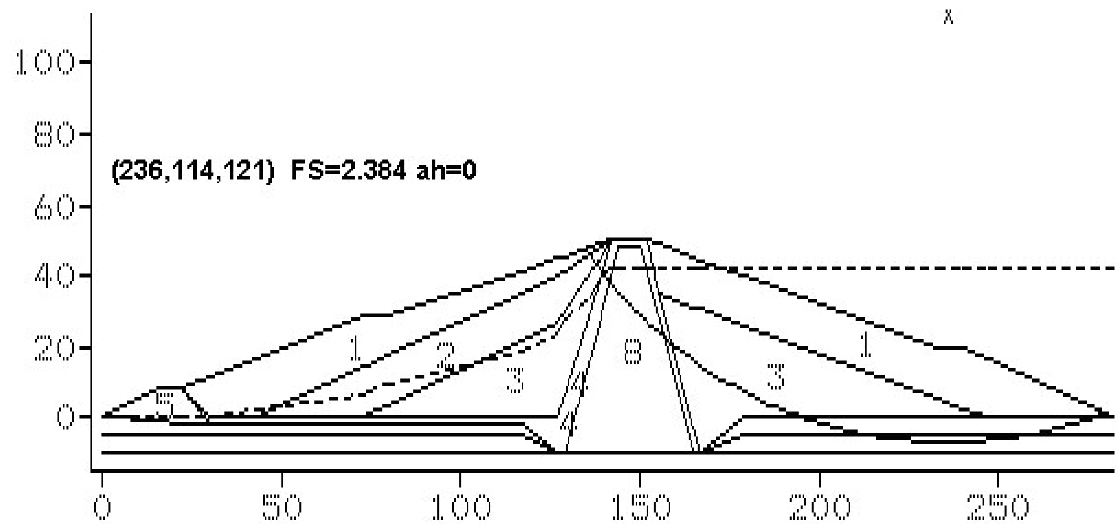

Figure 4.7 Trial circle no. 4 for Upstream Face

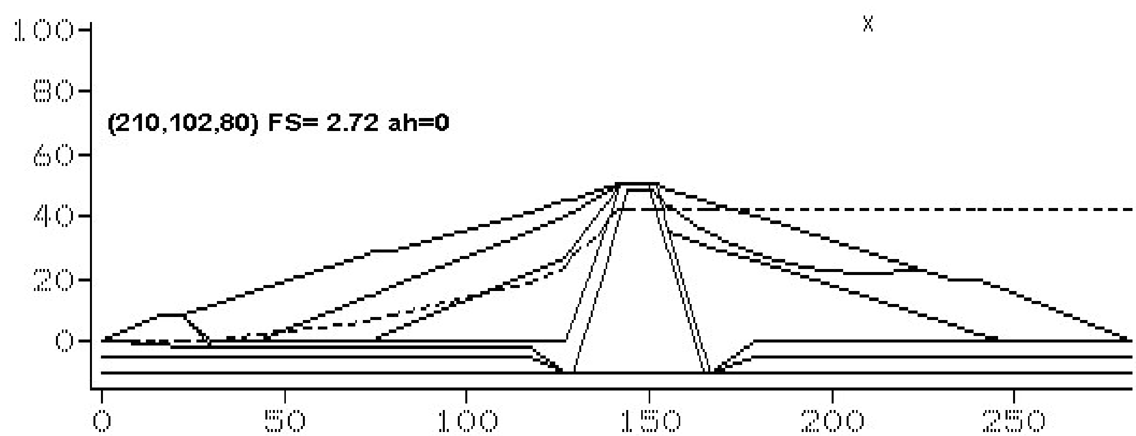

Figure 4.8 Trial circle no. 6 for Upstream Face

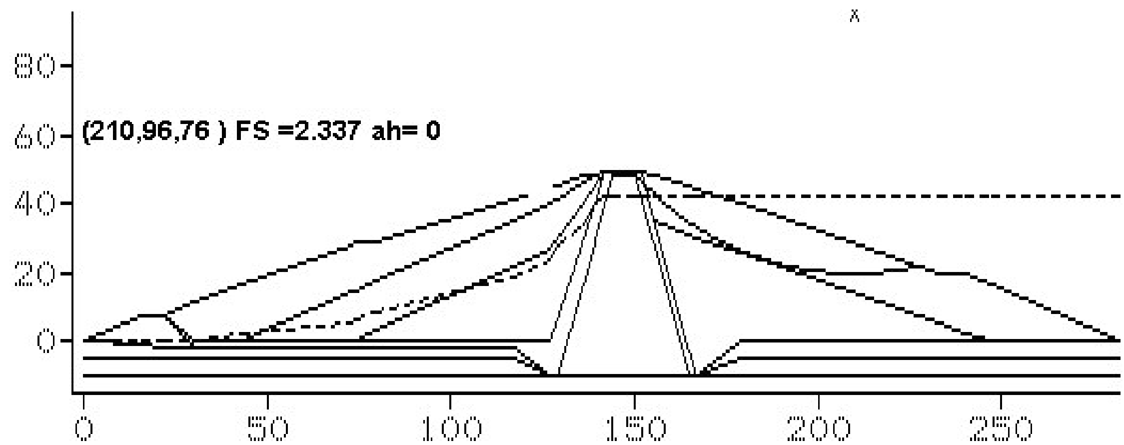

Figure 4.9 Trial circle no. 3 for Upstream Face

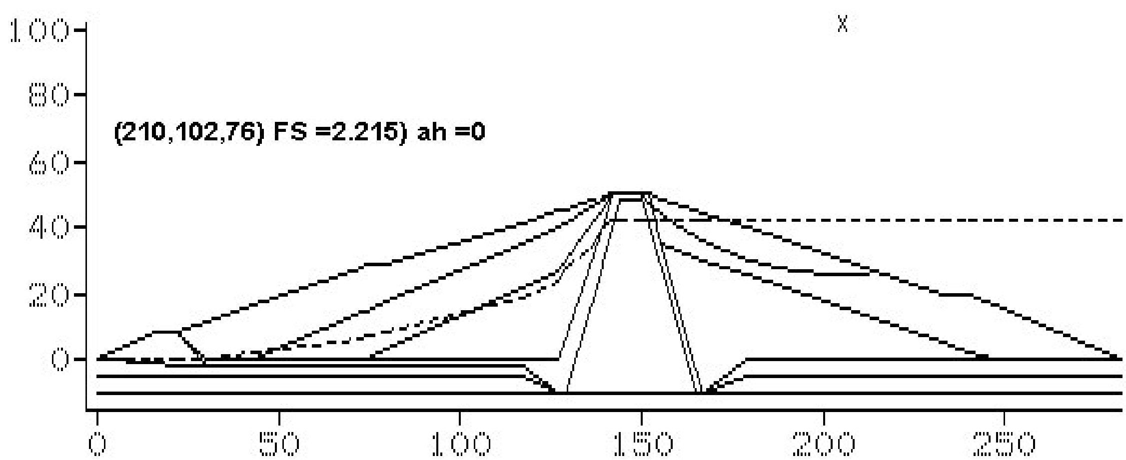

Figure 4.10 Trial circle no. 1 for Upstream Face

As it can be seen from table 4.1 and the above figures upstream face is much more critical according slope stability analyses so, yield acceleration and permanent displacement analyses of slip surface number 1(figure 4.10), for the upstream slope was taken into consideration. The minimum critical acceleration which gives a FS=1 was found to be 0.22 g

4.3. Static analysis of Nahrain Dam

Static analysis of Nahrain Dam is carried out in order to determine the state of stresses within the dam body prior to earthquake. This analysis was a mean to find dynamic material properties of dam body. To calculate the stresses, computer programs SAP90 and SAP 2000 were employed.

The model used in the analyses consists of 560 finite elements and 610 nodes. Figure 4.12 shows the model used for this purpose.

Since soil in general and dam materials especially have non-linear stress-strain relationships and SAP programs do not consider the non-linearity of these materials, in order to determine the static modulus of elasticity, an iterative procedure is employed. In this procedure elastic modulus of the elements are determined according to the following general formula (Hicher, 1996):

$$E = a\,(\sigma'_m)^n \qquad (4.1)$$

in which E is elastic modulus; a is a function of void ratio; σ'_m is mean effective stress determined as:

$$\sigma'_m=(\sigma'_1+\sigma'_2+\sigma'_3)/3 \qquad (4.2)$$

Four iterations were carried out and the maximum difference between the last two consecutive iterations was found to be 4.5 percent. Maximum allowable difference is accepted as 10 percent. Here parameters a and n are determined experimentally. In this study the following relationships derived from the formula 4.1 are used (Hicher, 1996).

For sand and gravel

$$E = \frac{450}{e_{sand}}(\sigma' m)^{1/2} \qquad (4.3)$$

For clay

$$E = \frac{450}{e_{clay}}(\sigma'_m)1/2 \qquad (4.4)$$

Where σ'_m is mean effective stress in (Mpa), where, e is void ratio, E is Young's modulus in terms of Mpa.

As it can be seen from 4.11 the value of Young's modulus differs significantly for different parts of the dam body. The inner and the lower parts of the dam have higher values of elastic values. Mainly there are three different types of material existing in the dam body. The dam (the embankment) are divided into thirty zones, and elastic modulus parameters are calculated for each zone. To calculate the effective stresses within the elements, hydrostatic pressure should be considered. Hence a total stress analysis was performed and by subtracting the pore pressures from total stresses at saturated zones effectıve stresses were found. Upstream part and the clay core were assumed as saturated and downstream part was assumed as wet. The effect of hydrostatic pressure was represented by introducing nodal forces that are increased with the increasing depth at the upstream face. (Figure 4.15)

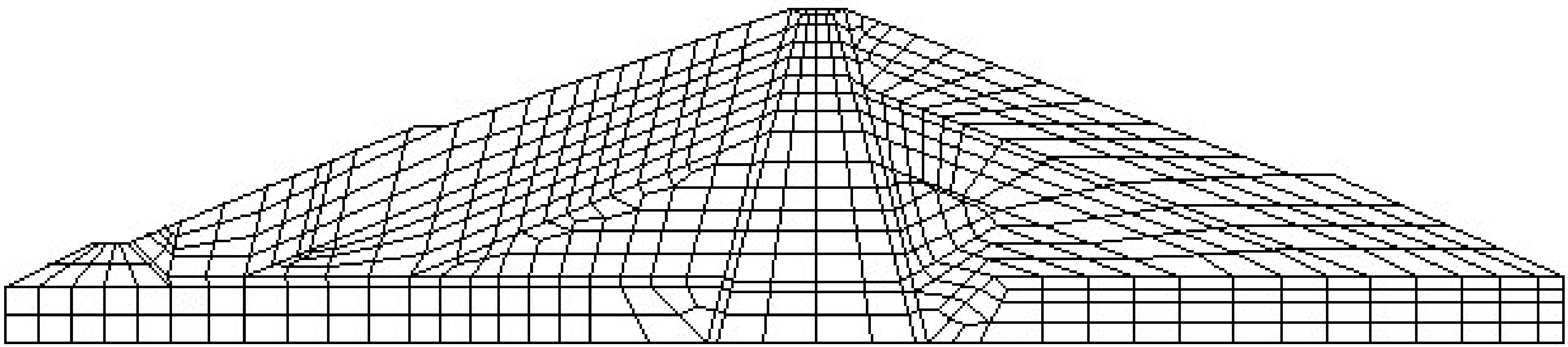

Figure 4.11 Model used for Static analysis of Naharin Dam with 560

finite elements and 610 nodes. 4.4. Dynamic material properties

Dynamic material properties are strain dependent shear modulus and damping whose accuracies are very important for determining the response of the dam correctly. Maximum shear modulus, G_{max} value can be directly be evaluated from measured shear wave velocity or from laboratory test conducted at low strains. Because of the cost and difficulty of measuring shear wave velocity, investigators have attempted to develop simple correlations to estimate shear wave velocity, V_s or maximum shear modulus, $G_{max.}$ Seed and Idriss (1970) suggested that shear modulus for sand could be estimated as:

$$G_{\max} = 1000 \times (k_2)_{\max} * (\sigma' m)^{0.5} \qquad (4.5)$$

Where σ'_m is the mean effective stress in lb/ft^2 and $(K_2)_{max}$ is a coefficient dependent on relative density that varies from 30 for loose sand to 75 for dense type.

In this study maximum shear modulus for sand and gravel is estimated by empirical (EQ.4.6) introduced by Richard and for clay using (EQ.4.7) suggested by Ohmachi and Kuwano (1994).

$$G_{\max} = 700 \times \frac{(2.17 - e)^2}{(1 + e)} (\sigma'_m)^{0.5} \qquad (4.6)$$

$$G\max = 3270 \times \frac{(2.97 - e)}{(1+e)} (\sigma'_m)^{0.5} \qquad (4.7)$$

The values of void ratio and for clay and sand materials used in dynamic analyses are shown in table 4.2.

Table 4.2 Void ratio and Poisson's ratio of construction material

Material type	**Average void ratio**	**Poisson' ratio**
Clay	0,35	0,39
Sand And Gravel	0,47	0,34
Filter	0,47	0,34
Riprap	0,42	0,30
Rock	0,35	0,37

4.5 Dynamic Analyses Of Nahrain Dam

Dynamic analysis of the Nahrain Dam was done by TELDYN program (Pyke, 1984). This program is a plain strain finite element program. The program uses equivalent linear method which involves an iterative computation in order to obtain shear moduli and damping ratios in each element which are compatible with average shear strain. This program automatically calculates the maximum shear modulus by using the following formula:

$$G_{max} = K_G \, P_a \, (\sigma'_m/P_a)^{ng} \qquad (4.8)$$

Where σ'_m is mean effective stress, p_a is atmospheric pressure, K_G and ng are dimensionless coefficients.

Shear modulus and damping curves used for sand and gravel and clay are shown in figures 4.12 and 4.13.

Further information about input and output options of the program can be found in appendix B.

The finite element model used for dynamic analysis is the same as the model used for static analysis (Figure 4.11). The model consists of 560 elements and 610 nodes. Material properties were taken from table 4.3 and table 3.1. Unit weights of the upstream and down stream were taken as saturated and wet respectively. The program uses following procedure:

First a set of shear moduli and damping values are estimated for each soil element of the finite element model. The system is analysed using these properties and the shear strain history is computed for each element. From these time histories the effective shear strain amplitudes are estimated for each element and the strain dependent shear moduli and damping of soils are consulted to check if the strain level is compatible with the values for shear moduli and damping used in the response evaluation. If the soil properties are not compatible, values of shear moduli and damping for the next iteration are improved and the process is repeated until convergence has occured; usually within 3 to 5 iterations. The response from the last iteration is taken as being the nonlinear response. The effective shear strain used during the analyses are taken as % 65 of the maximum shcar strain of the shear strain time history of each element.

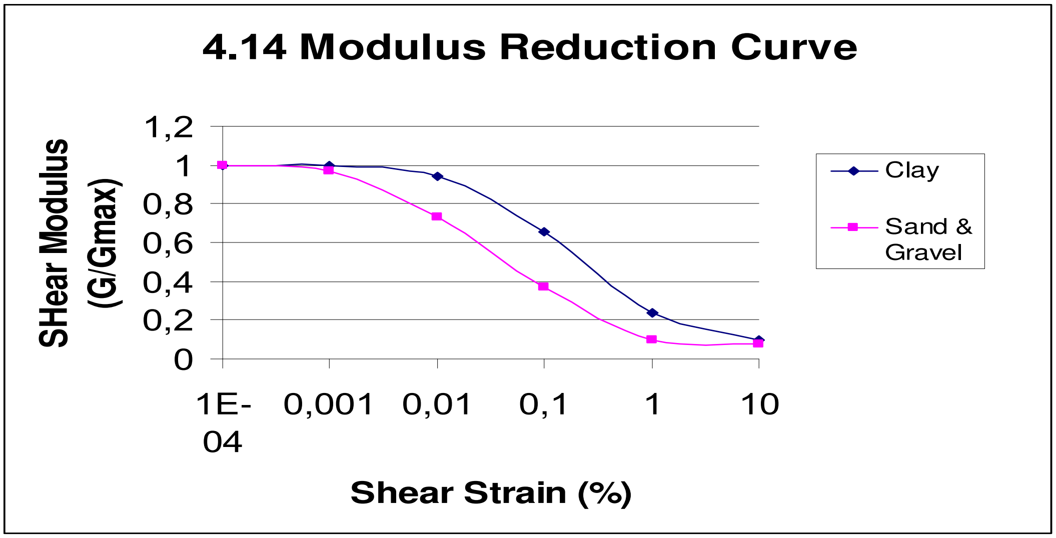

Figure 4.12 Modulus Reduction

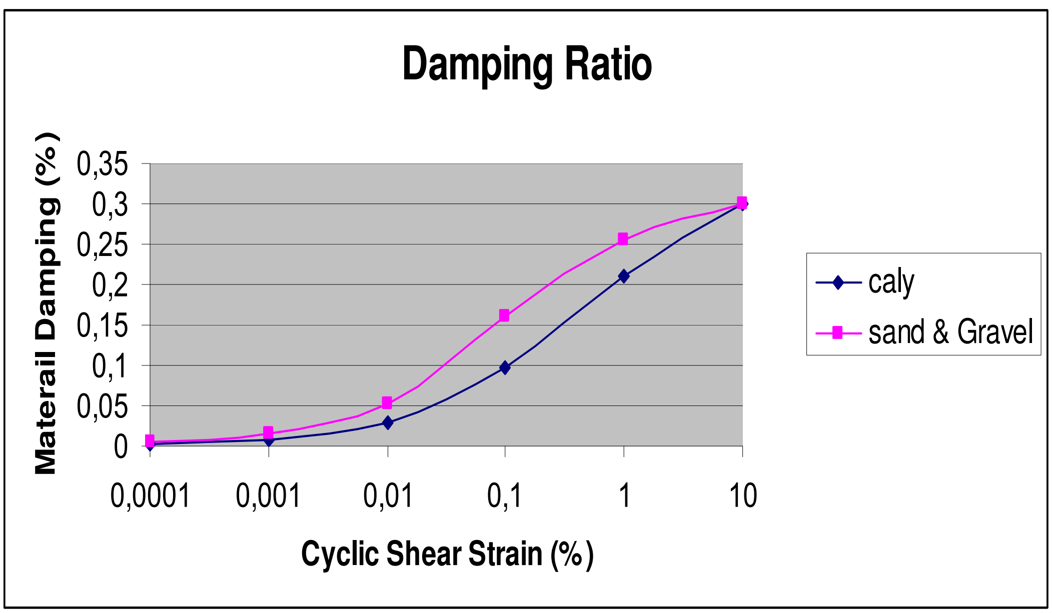

Figure 4.13 Damping Ratio Curve

.4.6 Permanent Displacement Analysis of Nahrin Dam

For the permanent displacement evaluation, time history of the average acceleration acting on the slip surface was determined by using the accelaration time histories of each node in the elements of the whole sliding block. As an input motion 1978 Tabas and 1968 Dayhok strong motion data(Ramzi, 1997) were used. (Figure 4.14) Then the corrected accelaration is calculated by subtracting the yield acceleration from each step of the average acceleration time history. Next, velocity history is obtained from corrected acceleration time history by integrating once and finally the permanent displacement of the slip surface is obtained by integrating the velocity time history once.

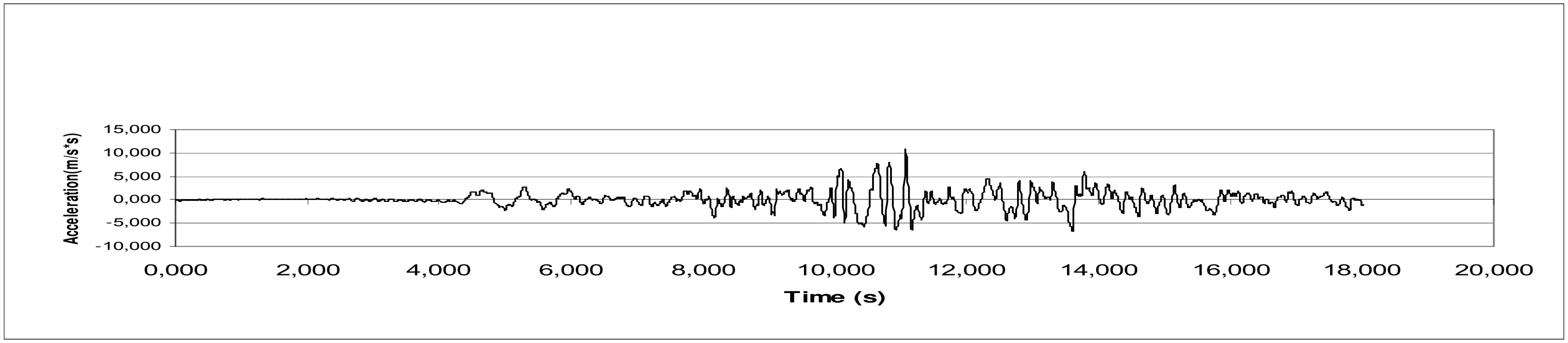

(a)

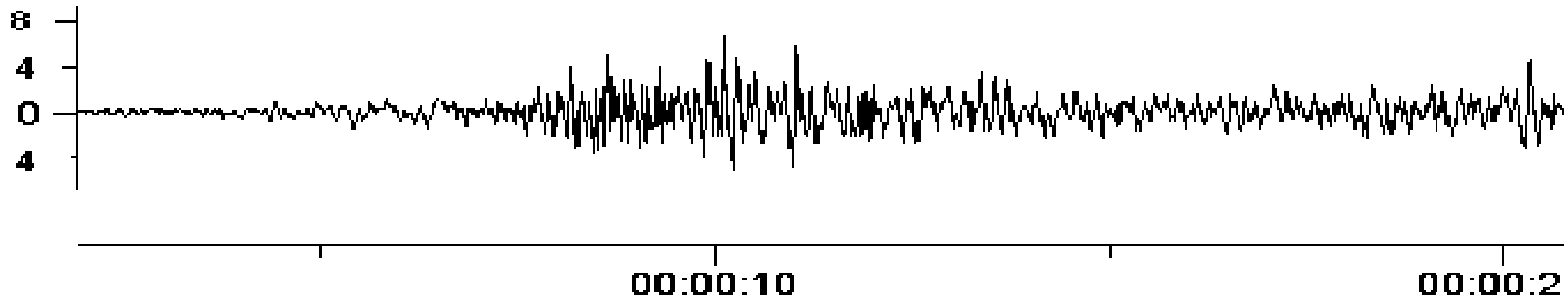

(b)

Figure 4.14 Acceleration Time Histories of (a) Bayhok (Ramzi, 1996), (b) Tabas

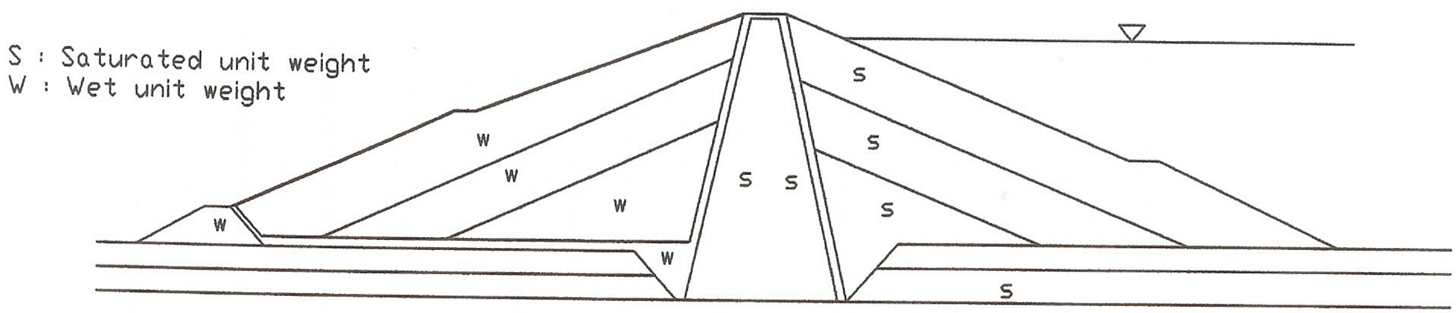

Figure 4.15 Saturated and Wet Parts of the Dam Body Assumed for Total Stress Analysis

Chapter V

Results Of the Dynamic Analysis Of Nahrain Dam

5.1 Distribution of Acceleration in the Dam Body

The acceleration time histories of nodes along the vertical axis of the dam were obtained from the dynamic analyses for each input motion. The selected nodes can be seen in Figure 5.1. Maximum acceleration versus height for each motion is shown in Figures 5.1 and 5.2. As it is seen from the figures the maximum accelerations are increasing from bottom to top. At the crest part of the dam it reaches to the maximum value. Roughly, maximum acceleration is stable through 2 / 3 of the dam height, however, at the top one-third of the dam height there is a significant increase in the maximum acceleration value. Ohmachi and Kuwano (1994) stated that the top part of the dam vibrates more than the bottom parts, so the crest should be designed in detail to avoid any deformation. These nodes are shown in figure 4.5. Fundamental period of the dam under small strains was found to be 0.71 second by fınıte elemnet program TELDYN.

5.2 Results of Permanent Displacement Analysis Of Nahrain Dam

Permanent displacement analyses of Nahrain Dam were carried out for two ground motions using the Newmark's (1965) procedure. Both ground motions were scaled to 0.26g Maximum permanent displacement of critical surface of dam was calculated as 32,49 cm (figure 5.3). This value was calculated for Tabas earthquake (1978) with Ms magnitude of 7.33. For the Bayhok (1997) the second selected base motion having a magnitude of Ms =7.1, max permanent displacement was calculated as 30.7 cm. Hyness-Griffin and Franklin (1984) have suggested the tolerable upper limit for the permanent displacement of the dam embankments as 100 cm. Therefore it can be said that the dam can stand this amount of displacement.

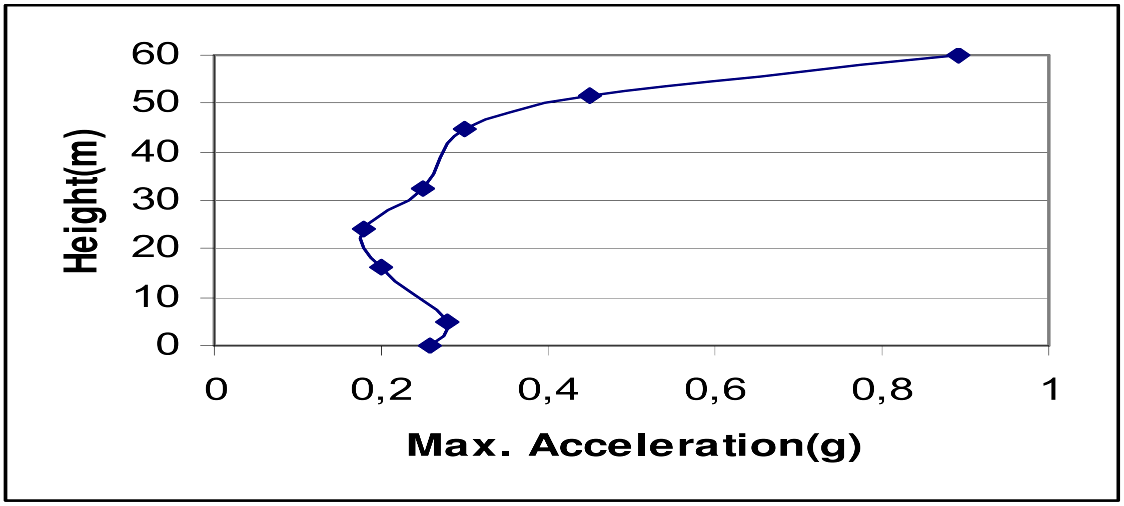

Figure 5.1 Maximum Acceleration Distribution throughout Selected nodes on the Dam Axis for Earthquake No. 1

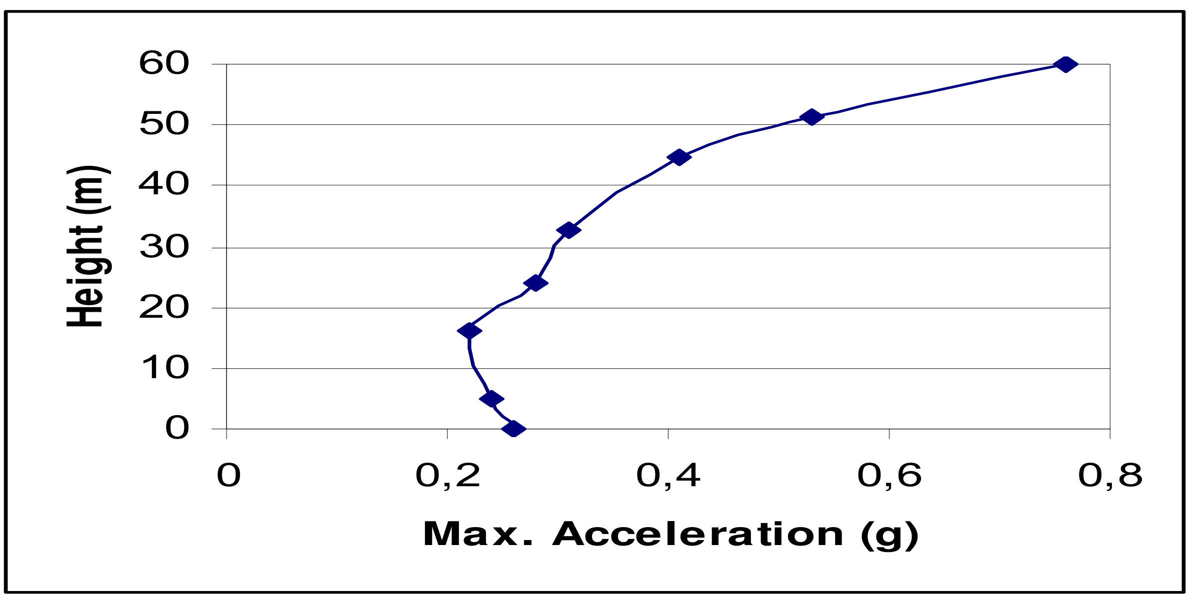

Figure 5.2 Maximum Acceleration Distribution throughout Selected nodes on the Dam Axis for Earthquake No. 2

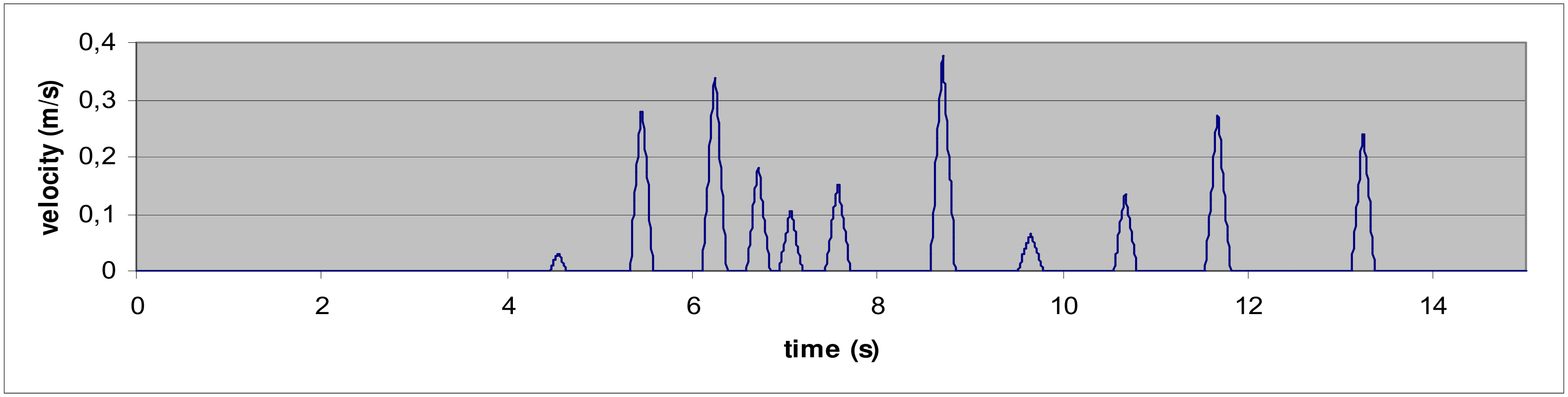

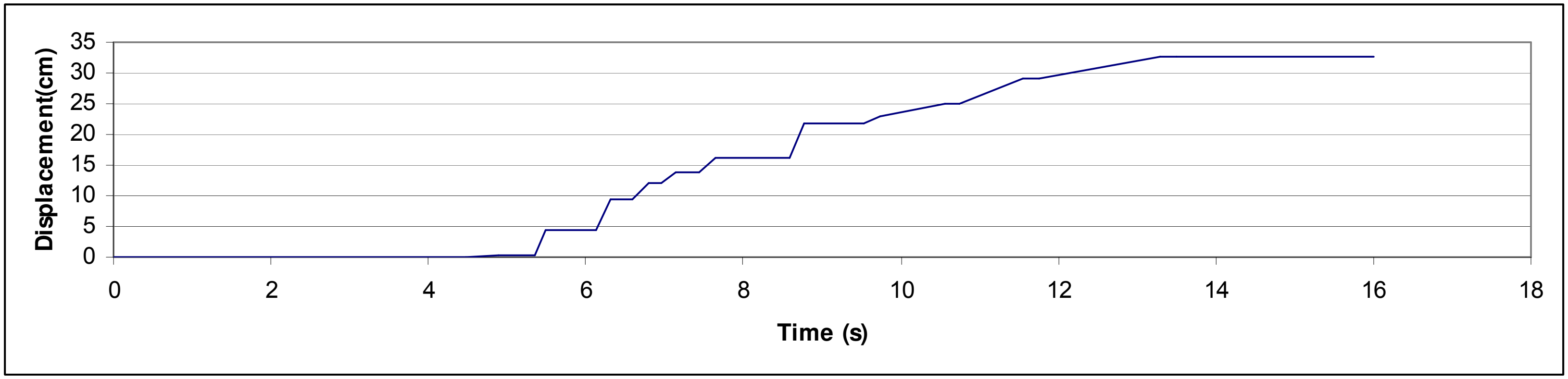

Figure 5.3. Permanent Displacement Time History of Critical Slip Surface considering Tabas Earthquake

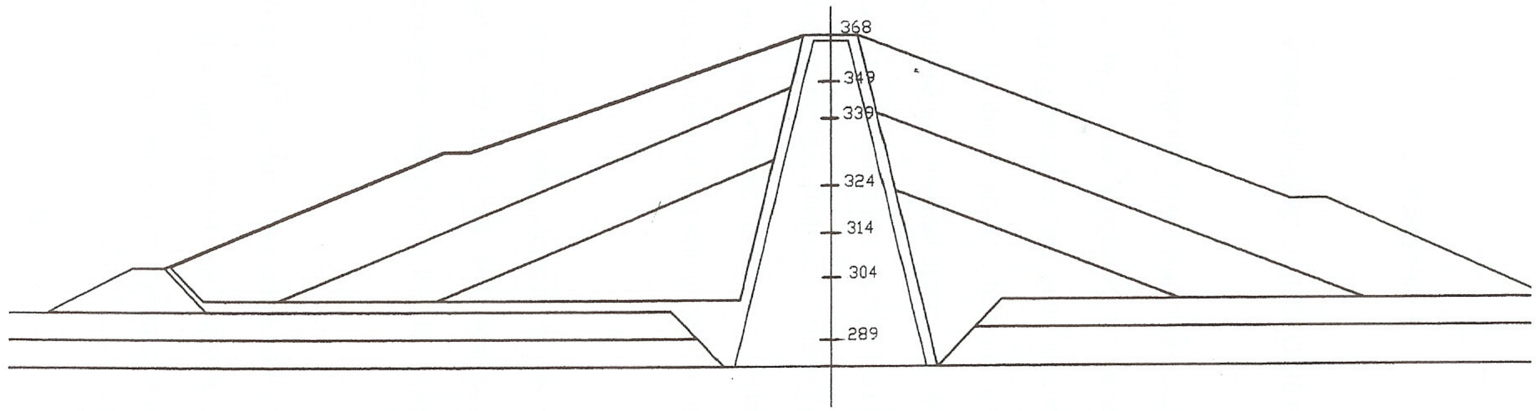

Figure 5.4 Selected Nodes Along Vertical Axis of Nahrain Dam

Chapter VI

SUMMARY AND CONCLUSION

The design of NAHRAIN DAM had been completed in mid 1990's, and the pseudo-static analysis was employed for seismic design. Safety of dam against sliding during earthquakes has been investigated using Pseudo-Static method of analysis. In this method, dynamic effect of the earthquake is represented by horizontal and vertical static driving forces on the sliding block. In the present study, the critical slide surface and yield acceleration of sliding block were determined by this method and only horizontal acceleration of ground motion was taken into consideration. Minimum static factor of safety was calculated to be 2.215 and regarding yield acceleration was determined as 0.22g.

Lifetime of the dam was planned to be 50 years. Considering the pervious earthquakes, different risk and nearest distance of the dam from governing fault, design acceleration at the dam foundation was determined as 0.26g (NDAR,1994).

Static analysis of the dam was done using SAP90 and SAP2000 finite element program. The main aim of this analysis was the estimation of initial material properties of the dam prior to dynamic analysis. In this step since, the programs do not consider the non-linearity of the materials, an iterative procedure was followed to determine modulus of elasticity. The finite element model used for the static analysis was in two-dimensional which represents plane strain case. Calculations of confining stresses were carried out according to effective stresses analyses for the full reservoir case. Results of this analysis are shown in appendix C.

Dynamic analysis of the dam was done using the finite element program TELDYN prepared for plane strain case. The model used for this part and that of previous section is the same. Dynamic material properties, input motions i.e. acceleration time history of the scenario earthquakes and other necessary data was entered as input to the program and the analyses was carried out. Results of this step and the other studies show that the maximum accelerations were experienced at the near the crest of the dam. As a result near crest upper downstream and upstream parts of the dam are more susceptible to seismic excitation and potential sliding.

Newmark's (1965) permanent displacement analysis was employed to predict maximum displacement of the sliding block subjected to scenario earthquakes. It was found that the critical block near the crest of the upstream side would experience a maximum of 34.5 cm displacement during an earthquake with a maximum acceleration of the 0.26g having the magnitude of Ms=7.33. This amount of displacement is in the allowable range.

The dam had been designed by pseudo-static analysıs method,using a maximum horizontal acceleration of 0.26g. As a matter of fact, many dams designed by using this technique has withstood earthquake motions satisfactorily. However, pseudo-static method has serious limitations and does not predict the permanent deformations caused by strong motions.

In the present study, static analysis of dam was done by using SAP 90 and SAP 2000 Finite element program and yield acceleration corresponding the critical slope was found to be 0.22g.

Permanent displacement analysis of Newmark is a powerful tool for determining the earthquake induced plastic deformations in an embankment. Saturation of the upstream part of the dam due to reservoir may cause greater reduction of shear strength as compared to that of downstream part. Also, at the top of an embankment dam the shear strength of the soil is lower than that of the soils at inner and / or lower parts of the dam, because the mean effective stresses are smaller at the top region than those at inner or lower regions. Additionally the accelerations are amplified near the crest of the embankment. All these show that the upstream part of crest has more tendencies to subject to permanent displacements.

The dynamic analyses of Nahrain Dam under the scenario earthquakes show that the critcal slip surface near the crest at the upstream side of the dam may have a permanent displacement of about 30 cm, as calculated by Newmark‘s method.

REFERENCES

Baba , K. 1982. ”On a Consideration for a Non-linear Analysis of Rockfill Dams”, Turkish National Committee for Earthquake Engineering, 9th Regional Seminar on Earthquake, September 7-17. Istanbul.

Borin, D.L., 1983. “SLOPE, Slope Stability Analysis Program”, Geosolve.

Clough, R. W., 1960. “The finite element method in plane stress analysis”, 2nd Conference on Electronic Computation, A. S. C. E., New York.

Fell R., MacGregor P., Stapledon D., 1992, Geotechnical Engineering of Embankment Dams.

Gazetas, G, 1987. “Seismic response of earth dams; some recent developments. ”Soil Dynamics and Earthquake Engineering, Vol. 6, No. 1, pp. 3-47.

Hatanaka, M. 1952. ”3-dimensional consideration on the vibration of earth dams,” Journal of the Japanese Society of Civil Engineers, Vol. 37, No. 10.

Hicher, P., 1996." Elastic Properties of Soils", Journal of geotechnical Engineering," ASCE, Vol. 122, No.8, pp, 641-648.

Hyness-Griffin, M. E., Franklin, A.G., 1984. "Rationalizing the Seismic Coefficient Method", Miscellaneous Paper GL-84-13, US Army Corps of Engineers, Washington, DC 20314.

Idriss, I.M., Lysmer, J., Hwang, R.N., and Seed, H.B., 1973. "QUAD-4: A Computer Program for Evaluating the Seismic Response of Soil Structures by Variable Damping Finite Element Procedures", Report No. EERC 73-16, Earthquake Engineering Research Center, University of California, Berkeley.

Idriss, I. M. and Duncan, James Michael, 1988, "Earthquake Response Analysis of Embankment Dams," Advanced Dam Engineering for Design, Construction, and Rehabilitation, Jansen, Van Nosthrand Reinhold.

Kramer, S, 1996. Geotechnical Earthquake Engineering, Prentice Hall, Upper Saddle River, New Jersey.

Lee, K.L, and Idriss, I.M, 1975. “Static Stresses by Non-Linear Methods”, Journal of Geotechnical Engineering Division, ASCE,VOl. 101,No. GT9, PP.871-887.

Lysmer, J., Udaka, T., Seed, H.B., and Hwang, R.N., 1974. “LUSH: A Computer Program for Complex Response Analysis of Soil-Structure Systems”, Report No. EERC 74-4, Earthquake Engineering Research Center, University of California, Berkeley.

Lysmer, J., Udaka, T., Tsai, C.F. and Seed, H. B., 1975. “FLUSH: A Computer Program for Approximate 3-D Analysis of Soil-Structure Interaction Problems”, Report No. EERC 75-30, Earthquake Engineering Research Center, University of California, Berkeley.

Marcuson, W. F., 1981. “Moderator’s report for session on Earth Dams and Stability of Slopes under Dynamic Loads”, Proceedings, International Conference on Recent Advances in Geotechnical Earthquake Engineering and Soil Dynamics, St. Louis, Missouri, Vol. 3, p. 1175.

Mohajer-Ashjai, A. & Nowroozi, A. A., 1978. Observed And Probable Intensity Zoning Of Iran. Tectonophysics, 29: 149-160

Mononobe. H. A. ET AL.1936. “Seismic stability of the earth dam,” Proceedings, 2nd Congress on Large Dams, Washington, D.C.,Vol.4.

NDAR, Nahrain Dam Analysis Report” ,1994, Ministry of Electricity and Water Resources of I. R. IRAN,. “

Newmark, N.M., 1965. “Effects of Earthquakes on Dams and Embankments”, Geotechnique, Vol.5, No.2.

Ohmachi, T., and Kuwano, J., 1994. “Dynamic Safety of earth and Rockfill Dams,” A.A. Balkema, Rotterdam.

Özkan, M.Y., 1998. “Review of Considerations on Seismic Safety of Embankment and Earth and Rock-Fill Dams”, Soil Dynamics and Earthquake Engineering, Vol. 17, pp. 439-458.

Pyke, R., 1984. “TELDYN, A Computer Program for Plane Strain, Dynamic Finite Element Analyses of Soils and Simple Structures, Users Manual”, TAGA, Engineering Software Services.

Ramzi, H.R., 1997. Accelerograms Data of the Iranian Accelerographs Network. Building and Housing Research Center Publications Tehran, Iran

Rowlins, Kyle M. Evans, Mark D. Diehl, Nathan B. and Daily William D.1998."Shear Modulus and Damping Relationships for Gravels." Journal of geotechnical and Geoenvironmental Engineering.

Seed, H.B., 1979. "Considerations in the Earthquake-Resistant Design of Earth and Rockfill Dams" Geotechnique, Vol.29, No.3, pp. 215-263.

Seed H. B, and Idriss, I. M,1970. "Soil Moduli and Damping Factors for Dynamic Response Analysis", Report No. EERC 70-10, Earthquake Engineering Research Center, University of California, Berkeley, California.

Seed, H. B. Lee, K. L, Idriss, I. M, and Makdisi, F. I, 1973. "Analysis of the Slides in the San Fernando Dams During the Earthquake of February 9,1971." Report No. EERC 73-2, Earthquake Engineering Research Center, University of California, Berkeley, California

Seed, H.B,1979. "Considerations in the Earthquake-Resistant Design of Earth and Rockfill Dams" Geotechnique, Vol. 29, No. 3, pp. 215-263.

Seed, H.B, Wong, R. T., Idriss, I. M. and Tokimatsu, K., 1984. "Moduli and Damping Factors for Dynamic Analyses of Cohesion less Soils", Journal of Geotechnical Engineering, ASCE, Vol. 112, No. 11, pp. 1016-1032

.Seed, H. B. 1986." Design problems in soil Liquefaction," Journal of Geotechnical Engineering, ASCE, Vol. 113, No. 8, pp. 827-845

Simons R. , (1979): Mainshock location and magnitude determination using combined U.S. and Mexican data; in the U.S.G.S. Prof. Paper 1254.

Walker Richard, 1995 Thrust faulting in eastern Iran: source parameters and surface deformation of the 1978 Tabas and 1968 Ferdows earthquake sequences. R. Walker, J. Jackson and C. Baker, *Geophysical Journal International, 152, 749-765*

Wasti, S. Tanvir and Utku, Mehmet 2001, "Introduction to Finite Element, Lecture Notes," Middle Technical University.

Wilson, E.L., and Habibullah, A., 1992. SAP90-A Series of Computer Programs for the Finite Element Analysis of Structures-Structural Analyses Users Manual", Computers and Structures, Inc., Berkeley, California.

Wilson, E.L., and Habibullah, A., 2000. SAP 2000 Series of Computer Programs for the Finite Element Analysis of Structures-Structural Analyses Users Manual", Computers and Structures, Inc., Berkeley, California.

Appendix A

List of major earthquake within 300 km distance from Nahrain Dam

Year	Month	Day	Time	Latitude	longitude	Depth (km)	Mb	Ms	Reference
1903	3	22	143500	33.16	59.71	15	6.2	6.2	AMB
1903	9	25	120000	35.18	58.23	15	5.3	5.9	AMB
1909	9	27	0	30.09	57.58	15	5.5	0	KAR
1910	10	27	184500	30.09	57.58	15	5.5	5.5	AMB
1911	4	18	181400	31.32	57.03	15	6.2	6.2	AMB
1911	4	29	53300	30.36	57.58	15	6.2	5.6	AMB
1916	2	11	205320	36	59.5	7	5	4.6	WDC
1923	5	25	222100	35.19	59.11	15	5.8	5.8	AMB
1923	5	25	222100	35.19	59.11	15	5.7	5.8	AMB
1925	12	14	11	34.6	58.1	15	5.4	5.5	WDC
1928	4	14	131644	35.3	54.4	15	5.2	0	CP
1928	8	21	190200	35.5	59	12	5	0	CP
1932	9	8	72500	31.59	58.15	15	5.6	5.6	AMB
1933	10	5	132900	34.52	57.07	15	6.2	6	AMB
1933	11	28	110900	32.01	55.94	15	6.4	6.2	AMB
1935	4	15	230435	35.9	54.9	12	4.2	0	CP
1935	4	15	230435	35.9	54	70	4.9	4.4	WDC
1939	4	6	40800	35	54.4	15	5.6	0	ISS
1939	6	10	83641	34.2	56.6	15	5.6	0	ISS
1940	5	4	210100	35.76	58.53	12	6.2	6.4	AMB
1949	12	14	34350	36	59	12	5	0	ISS
1949	12	14	34350	36	59	12	5.1	4.8	WDC
1951	6	17	184623	35.7	57	15	4.5	0	ISS
1953	1	15	200800	31.07	56.78	15	5.6	5.5	AMB
1953	2	12	81500	35.39	54.88	33	6.9	6.5	AMB
1953	2	13	43628	35.6	54.7	15	4.5	0	CP
1953	4	1	22435	35.5	55.2	15	4	0	CP
1953	6	6	224	35.3	58.6	13	4.6	0	WDC
1953	6	6	224	35.6	59	15	4.5	0	CP
1953	7	11	152508	35.9	55.1	15	4.5	0	CP
1953	7	24	162930	35.5	55	15	4.7	0	CP
1958	1	28	171500	35.8	58.1	12	4.7	0	CP
1958	1	22	0	35.6	58.7	12	4.9	4.3	WDC
1958	2	27	35600	35.3	58.9	12	4.7	0	CP
1954	9	16	142230	34.5	59.5	15	5.1	0	USA
1959	10	14	72800	35.5	59.5	12	4.5	0	CP
1960	1	6	225652	32	54.5	15	5	0	FS
1960	3	7	5140	34.5	55	15	4.3	0	USA

1962	10	16	0	35.2	58.3	12	5	0	WDS
1962	10	30	140300	35.5	56.8	10	3.5	0	RU
1963	1	1	192200	35.4	58.8	15	4.5	0	MOS
1963	1	1	192733	35.4	58.9	11	4.9	4.4	WDC
1963	3	1	32002	35.8	59.9	33	4.6	0	MOS
1964	3	1	31958	35.88	59.85	1	4	0	NA
1964	2	21	10356	34.51	58.06	15	4.8	0	ISC
1964	2	21	10358	34.54	58.07	6	5	0	NA
1964	2	21	10400	34.4	58.1	33	5	0	USGS
1964	5	15	223100	35.9	58.6	16	4.5	0	MOS
1964	8	10	181841	30.1	57.67	52	4.5	0	ISC
1964	8	10	181841	30.1	57.7	13	4.5	0	USA
1964	8	10	181835	30.3	57.7	13	4.5	0	USGS
1964	8	10	181834	30.05	57.72	1	4.5	0	NA
1964	11	3	61429	32.8	59.32	33	4.5	0	ISC
1964	11	3	61429	32.4	59.1	33	4.5	0	USA
1965	2	26	13707	35.24	57.54	33	5.1	0	ISC
1965	2	26	13705	35.1	57.6	33	5.2	0	USGS
1965	2	26	13707	35.2	57.5	33	5	0	MOS
1965	2	26	13700	35.09	57.88	1	5.2	0	NA
1965	5	4	184058	32.3	55.6	28	4.8	0	USA
1965	6	4	184055	32.32	55.54	15	4.8	0	ISC
1965	6	4	184058	32.4	55.5	18	4.8	0	USGS
1965	7	22	123022	36	57.9	15	3.5	0	ZS
1965	11	28	244946	36	56	15	4	0	MOS
1966	6	13	10353	32.2	54.4	56	4.8	0	USGS
1966	8	30	64226	32.2	56.1	33	4	0	USA
1967	3	2	75525	31.98	55.87	37	4.7	0	ISC
1967	3	2	75525	32	55.8	33	4.9	0	USGS
1967	3	2	75524	32.1	55.8	33	4.6	0	USA
1968	8	30	211120	34.9	59.5	33	4.3	0	USGS
1968	8	31	104737	34	59	13	7.3	7.4	USGS
1968	8	31	104742	34.02	58.96	18	7.3	7.4	AMB
1968	8	31	113433	34	59.19	26	5.4	0	ISC
1968	8	31	113433	33.9	59.2	24	5.5	0	USGS
1968	8	31	132257	34.11	59.49	13	4.7	0	ISC
1968	8	31	132260	34.1	59.4	33	4.8	0	USGS
1968	8	31	140616	34.08	59.44	17	4.9	0	ISC
1968	8	31	140616	34.1	59.4	18	5	0	USGS
1968	9	1	72730	34	58.2	15	5.9	6.3	WDC
1968	9	1	72700	34.05	58.23	15	5.9	6.4	AMB
1968	9	1	72730	34.09	28.24	14	5.9	0	ISC
1968	9	1	72730	34	58.2	15	5.9	6.3	USGS
1968	9	1	110358	34.2	29.9	2	4.9	0	ISC
1968	9	1	110402	34	59.6	33	4.8	0	USGS
1968	9	1	191637	34.16	58.24	20	4.8	0	ISC

1968	9	1	191637	34.2	58.3	23	5	0	USGS
1968	9	1	211645	34.4	58	44	4.8	0	USGS
1968	9	3	95347	33.8	59.2	16	5	0	USGS
1968	9	4	55408	35.1	58.5	33	4.7	0	USGS
1968	9	4	80845	34.2	59.47	24	5	0	ISC
1968	9	4	80844	33.9	59.2	24	5	0	USGS
1968	9	4	111936	34	59.31	25	5	0	ISC
1968	9	4	111935	33.9	59.1	25	5.1	0	USGS
1968	9	4	232445	34.6	58.32	1	5.2	0	ISC
1968	9	4	232447	34	58.2	15	5.2	0	USGS
1968	9	6	22736	34.6	59.52	16	4.7	0	ISC
1968	9	6	22737	34	59.3	27	4.9	0	USGS
1968	9	10	203158	34.8	59.49	10	4.7	0	ISC
1968	9	10	203158	34	59.4	18	4.7	0	USGS
1968	9	11	191714	34.03	59.54	33	5.2	0	ISC
1968	9	11	191713	33.9	59.4	31	5.4	0	USGS
1968	9	15	94214	34.03	59.59	14	4.8	0	ISC
1968	9	15	94214	34	59.4	20	4.9	0	USGS
1968	9	17	191509	34.1	58.37	38	4.4	0	ISC
1968	9	19	51516	34.4	58	48	4.6	0	USGS
1968	11	28	180246	34.23	59.65	33	4.8	0	ISC
1969	3	4	173549	31	57.8	59	4.3	0	USGS
1969	6	28	223213	32.38	56.26	9	4.5	0	ISC
1969	8	23	191818	33.9	58.9	32	5.1	0	USGS
1969	9	2	133007	30.22	57.74	53	4.9	0	ISC
1969	9	2	133003	30.2	57.7	20	5.3	0	USGS
1969	9	3	233902	34.11	58.16	31	4.9	0	ISC
1969	9	3	233903	34.3	58.3	33	4.8	0	USGS
1969	9	3	233902	34.1	58.3	15	4.5	0	MOS
1969	11	11	3035	33.43	54.94	35	4.9	0	ISC
1969	11	11	3035	33.4	55	33	5	0	USGS
1969	12	2	224616	34	58.76	40	5	0	ISC
1969	12	2	224615	33.9	58.6	33	5.1	0	USGS
1970	3	1	201242	34.05	58.95	15	5	0	ISC
1970	3	1	201245	34	58.9	39	5.2	0	USGS
1970	3	1	201240	34.1	59	15	5	0	MOS
1970	3	17	231944	34.04	59.74	25	4.9	0	ISC
1970	3	17	231942	33.9	59.7	19	5	0	USGS
1970	8	30	123132	30.8	57.2	15	4.5	0	MOS
1970	8	30	123132	30.8	57.2	13	4.5	0	MOS
1971	4	6	215556	30.0	54.9	15	4	0	MOS
1971	4	25	13048	35.2	59.2	15	4.2	0	MOS
1971	5	22	140203	35.66	58.23	15	4.7	0	ISC
1971	5	22	140207	35.6	58.3	36	4.8	0	USGS
1971	5	22	140203	35.7	58.2	15	4.6	0	MOS
1971	5	26	24146	35.55	58.2	25	5.4	0	ISC

1971	5	26	24100	35.5	58.3	19	5.8	5.6	AMB
1971	5	26	24146	35.5	58.2	26	5.4	0	USGS
1971	5	26	24142	35.5	58.2	15	5.9	0	MOS
1971	5	26	24147	35.5	58.3	15	5.7	0	BCI
1971	7	24	4919	30.39	59.81	35	4.9	0	MOS
1971	7	24	4921	30.4	59.9	56	5	0	USGS
1971	9	16	142033	34.9	58.1	15	4.9	4.3	WDC
1972	4	17	151240	31.8	59.24	19	4.1	0	ISC
1972	4	17	151243	31.9	59.3	44	4.5	0	USGS
1972	4	17	151243	32	59.2	44	4.8	0	MOS
1972	10	9	15812	30.06	57.72	83	4.8	0	ISC
1972	11	10	44509	30.25	57.66	11	4.6	0	ISC
1972	11	10	44511	30.3	57.6	33	4.7	4.2	WDC
1972	12	1	113903	35.48	57.92	25	5.2	0	ISC
1972	12	1	113903	35.4	57.9	33	5.4	5.2	WDC
1973	2	10	170750	31.82	56.17	63	4.7	0	ISC
1973	2	10	170747	31.9	56.1	42	4.5	0	USE
1973	2	22	224333	33	56	15	4.3	0	HFC
1973	5	3	61232	33.38	57.36	0	4.5	0	ISC
1973	5	5	61236	33.3	57.4	15	4.6	0	USE
1973	5	5	61230	33.3	57.4	33	4.6	0	WDC
1973	5	11	135220	33.41	57.48	22	5.1	0	ISC
1973	5	11	135232	33.4	57.4	50	5.1	0	USE
1973	5	17	161136	35.54	57.75	29	5	0	ISC
1973	5	17	161137	35.5	57.8	45	4.9	0	USE
1973	5	17	161136	35.6	57.8	20	5.1	0	MOS
1973	5	22	5014	35.3	57.1	45	5.1	0	WDC
1973	5	22	5011	35.2	57.2	20	5	0	MOS
1973	9	17	92111	30.44	59.85	33	4.6	0	ISC
1973	9	22	92111	30.5	59.9	15	4.6	0	USE
1973	9	22	92131	33	59	15	4.9	0	HFC
1973	10	27	142218	33	54	15	4.5	0	HFC
1973	11	20	22316	32.04	54.58	31	5	0	ISC
1973	11	20	23318	32	54.5	45	5	0	USE
1973	11	20	23315	32.1	54.6	15	5.2	0	MOS
1974	3	2	90150	33.3	58.4	33	4	0	ISC
1974	4	25	51144	30.6	56.5	0	4.1	0	ISC
1974	4	29	30719	32.6	58.6	24	3.1	0	USE
1974	6	17	72249	33.7	57	35	4.8	0	USE
1974	11	17	150548	32.8	55.1	43	5.2	0	USE
1975	4	28	20117	33.3	54.8	42	5.3	0	USE
1975	11	15	181905	32.11	54.49	43	4	0	USE
1975	11	15	182650	31.99	54.54	41	4	0	USE
1975	11	15	233955	32.12	54.46	44	3.7	0	USE
1975	11	30	160432	31.99	54.57	37	4	0	USE
1975	12	1	164554	35.1	59.99	35	4.1	0	USE

1976	3	31	233859	34.66	57.17	23	4.7	0	USE
1976	11	7	40000	33.82	59.19	15	5.8	6.4	AMB
1976	11	7	40052	33.8	59.16	13	5.7	6.2	WDC
1976	11	9	175954	33.79	59.23	29	5.1	0	USE
1976	12	31	211033	31.28	54.51	62	4.4	0	USGS
1977	4	2	221611	32.2	56.6	33	4.7	4.2	WDC
1977	5	3	162658	31.7	56.2	42	5	4.6	WDC
1977	9	17	52506	30.9	56.6	33	4.8	0	WDC
1977	11	10	135235	34	59.4	23	4.7	4.2	WDC
1977	11	10	140934	31.4	56.9	33	4.8	4.3	WDC
1977	12	19	233400	30.9	56.61	15	5.7	5.8	AMB
1978	5	22	61815	31.8	56.2	34	5	5.3	WDC
1978	5	23	113143	31.87	56.17	25	5	0	USGS
1978	9	16	153600	33.4	57.12	15	6.7	7.3	AMB
1978	9	16	153556	33.38	57.43	33	6.5	7.4	USGS
1978	9	16	182547	33.78	57.19	33	4.6	0	USGS
1978	9	16	184514	33.87	57.8	16	4.8	0	USGS
1978	9	16	195021	33.72	57.11	33	4.9	0	USGS
1978	9	16	220713	34.94	57.11	33	4.5	0	USGS
1978	9	17	73550	33.14	56.93	33	4.7	0	USGS
1978	9	17	81724	33.66	57	33	5	0	USGS
1978	9	17	124325	34.12	57.57	33	4.7	4.1	USGS
1978	9	17	213945	33.74	57.23	33	4.2	0	USGS
1978	9	18	13448	33.68	57.2	33	4.5	0	USGS
1978	9	18	450020	33.53	57.3	23	4.7	4.2	USGS
1978	9	18	173508	33.69	56.92	33	4.9	0	USGS
1978	9	20	445580	33.18	58.65	33	4.3	0	USGS
1978	9	24	181604	33.56	57.16	33	4.5	3.7	USGS
1978	9	24	213138	33.28	57.25	58	4.3	0	USGS
1978	9	25	142623	33.2	57.15	33	3.9	0	USGS
1978	9	28	25033	34.27	56.81	43	4.3	0	USGS
1978	10	3	213610	32.82	57.37	33	4.2	0	USGS
1978	10	9	160442	33.39	57.29	33	4.5	3.6	USGS
1978	11	6	164955	33.4	57.4	11	4.6	4	WDC
1978	11	6	231409	33.6	57.1	33	4.6	4	WDC
1978	11	6	234642	33.2	54.9	33	4.7	4.2	WDC
1978	12	6	203809	33.2	57.1	20	4.6	4	WDC
1978	12	26	103523	33.67	57.24	45	4.5	0	USGS
1979	1	10	162816	33.5	57.2	33	4.7	4.2	WDC
1979	1	16	95010	33.89	59.47	33	5.9	6.7	USGS
1979	1	16	95000	33.8	59.5	19	6	6.8	AMB
1979	1	17	32949	33.75	57.09	33	5.1	0	USGS
1979	1	17	75243	34	59.42	33	4.7	0	USGS
1979	1	19	192945	33.9	59.4	33	5	4.3	WDC
1979	1	27	53244	34	59.68	10	4.4	3.7	USGS
1979	1	29	134924	33.91	59.38	33	4.6	0	USGS

1979	2	8	133608	34.05	59.53	10	4.4	0	USGS
1979	2	13	103616	33.31	57.43	33	5.5	4.8	USGS
1979	3	22	65540	33.33	57.28	33	4.1	0	USGS
1979	4	5	34534	33.45	57.01	33	4.6	0	USGS
1979	4	16	95010	33.9	59.47	33	5.9	0	USGS
1979	4	23	172417	33.87	59.47	16	4.6	0	USGS
1979	5	27	64315	33.23	57.25	10	4.7	3.9	USGS
1979	7	5	44612	33.7	57.11	33	4.7	0	USGS
1979	8	25	134625	33.51	58.99	15	4.2	0	USGS
1979	9	5	92654	33.8	56.95	33	5.2	0	USGS
1979	9	18	171631	30.56	54.61	33	4.2	0	USGS
1979	11	2	61049	33.64	57.35	33	4.8	0	USGS
1979	11	14	25017	33.89	59.79	33	4.9	0	USGS
1979	11	14	41828	34.08	59.57	33	4.8	0	USGS
1979	11	14	221000	33.91	59.81	15	6	6.6	AMB
1979	11	14	74340	33.85	59.92	33	4.6	0	USGS
1979	11	14	211059	33.92	59.71	33	3.7	0	USGS
1979	11	15	32529	33.82	59.66	42	4.8	4	USGS
1979	11	15	50660	33.92	59.82	33	5	4	USGS
1979	11	20	114112	33.87	59.61	10	4.1	0	USGS
1979	11	23	182248	33.98	59.83	33	5	4.5	USGS
1979	11	23	204800	34.04	59.79	10	3.9	0	USGS
1979	11	24	14640	33.91	59.74	33	4.3	0	USGS
1979	11	24	64504	33.91	59.72	33	4.1	0	USGS
1979	11	27	71236	33.97	59.84	17	5	0	USGS
1979	11	27	171033	33.96	59.72	10	6.1	7.1	USGS
1979	11	27	171000	34.05	59.63	15	6.1	7.1	AMB
1979	11	27	180458	33.96	59.47	10	4.6	0	USGS
1979	11	27	200016	34.02	59.54	10	4.4	0	USGS
1979	11	27	204824	33.9	59.9	10	4.3	0	USGS
1979	11	27	231456	33.77	59.37	10	4.4	4	USGS
1979	11	28	115551	34.02	59.7	10	4.2	0	USGS
1979	11	28	121203	34.07	59.46	10	4.2	0	USGS
1979	11	28	163841	34.03	59.31	10	4	0	USGS
1979	11	28	180914	34.06	59.93	10	4.4	0	USGS
1979	11	28	190949	34.11	59.69	10	4.2	0	USGS
1979	11	29	4858	33.97	59.35	36	4.4	0	USGS
1979	12	2	61049	33.64	57.05	33	4.8	0	USGS
1979	12	2	210938	34.01	59.58	33	4.2	0	USGS
1979	12	7	92400	34.03	59.81	31	5.8	6	USGS
1979	12	7	92401	34.23	59.88	33	5.8	6	USGS
1979	12	7	95449	34.03	59.9	27	4.8	0	USGS
1979	12	7	104508	34.1	59.75	33	4.6	0	USGS
1979	12	8	73113	34.07	59.91	33	4.2	0	USGS
1979	12	9	91207	35.05	59.81	48	5.2	5.3	USGS
1979	12	11	21659	33.78	59.65	33	4.4	0	USGS

1979	12	16	223540	33.99	59.32	33	5	4.7	USGS
1979	12	25	164404	34.08	59.79	10	4.9	0	USGS
1979	12	30	130802	33.73	55.24	33	4.6	0	USGS
1980	1	12	153142	33.49	55.19	33	5.4	5.9	USGS
1980	1	30	193625	34.04	59.33	10	4.6	4	USGS
1980	3	4	70816	33.92	59.48	33	4.2	0	USGS
1980	3	15	230856	33.76	59.92	33	4.3	3.7	USGS
1980	4	14	100430	33.94	59.44	33	4.6	0	USGS
1980	4	27	918038	34.24	59.48	33	4.3	0	USGS
1980	5	18	63026	34.05	59.62	32	4.7	3.6	USGS
1980	10	12	52747	33.97	59.33	42	4.4	0	USGS
1980	10	26	65037	34.01	59.52	33	4.5	0	USGS
1980	10	30	191518	35.61	58.66	33	4.4	0	USGS
1980	10	31	40651	35.96	58.56	33	4.6	3.9	USGS
1981	3	22	93417	34.03	59.33	33	4.5	0	USGS
1981	4	30	102127	33.13	57.16	33	4.5	0	USGS
1981	4	30	93931	33.1	57.03	35	4.3	0	USGS
1981	6	12	103224	30.13	57.39	33	4.4	0	USGS
1981	6	12	104515	30.01	58	33	4.6	0	USGS
1981	6	12	104501	30	58.12	33	4.7	0	USGS
1981	6	27	173125	31.13	57.33	33	4.7	3.6	USGS
1981	7	28	172200	30	57.8	33	6.2	7	WDC
1981	7	28	175019	30.12	57.01	33	4.3	0	USGS
1981	7	28	183028	30.23	57.48	33	4.7	0	USGS
1981	7	28	172225	30.01	57.79	33	6.7	7.1	USGS
1981	7	28	184834	30.12	57.46	33	4.5	0	USGS
1981	7	28	190555	30.17	57.45	33	4.9	0	USGS
1981	7	28	203256	30.04	57.64	33	4.2	0	USGS
1981	7	28	214523	30.03	57.65	33	4.9	0	USGS
1981	7	28	225648	30.23	57.52	33	4.4	0	USGS
1981	7	29	43316	30.12	57.73	33	4.7	0	USGS
1981	7	29	50445	30.14	57.49	33	4.7	0	USGS
1981	7	29	51143	30.58	57.49	33	4.6	4.3	USGS
1981	7	29	65919	30.18	57.52	33	4.4	0	USGS
1981	7	29	100923	30.26	57.31	33	4.2	0	USGS
1981	7	29	220327	30.32	57.35	33	4.4	0	USGS
1981	7	30	111452	30.47	57.57	34	4.5	3.7	USGS
1981	7	31	144357	30.61	57.31	33	4.4	0	USGS
1981	8	2	133727	30.18	57.64	33	4.6	0	USGS
1981	8	2	145039	30.52	57.91	33	4.2	0	USGS
1981	8	3	25545	30.03	57.55	33	4.6	0	USGS
1981	8	4	171453	30.08	57.53	33	4.5	0	USGS
1981	8	10	212920	30.02	57.67	33	4.1	0	USGS
1981	8	20	190208	30.12	57.51	27	4.6	4.2	USGS
1981	9	22	62657	30.01	57.56	33	4.3	0	USGS
1981	9	26	73325	30.23	57.58	33	4.8	0	USGS

1981	11	21	41044	33.53	57.46	47	4.5	0	USGS
1982	1	2	190049	30.65	57.51	33	5	0	USGS
1982	1	21	234250	30.17	57.65	33	4.4	0	USGS
1982	1	30	14660	30.37	57.74	33	4.4	0	USGS
1982	2	5	162859	30.72	57.4	33	4.4	0	USGS
1982	2	25	235159	30.13	58.01	33	4.6	0	USGS
1982	5	15	173609	35.47	54.01	32	4.5	0	USGS
1982	6	12	120340	32.05	55.7	33	4.8	3.6	USGS
1982	6	14	153349	30.12	57.66	33	4.7	0	USGS
1982	7	17	80806	30.15	57.34	31	4.3	0	USGS
1982	8	22	90321	33.21	54.92	33	4.6	3.7	USGS
1982	12	8	193421	30.62	57.6	40	4.8	0	USGS
1982	12	19	194053	30.57	57.52	35	5	5.9	USGS
1983	2	28	13735	30.03	57.81	33	4.2	0	USGS
1983	4	19	232	31.15	57.49	33	4.3	0	USGS
1983	5	1	230628	30.33	57.59	33	4.4	0	USGS
1983	5	3	5526	30.12	57.75	33	4.3	0	USGS
1983	5	3	133026	33.19	57.34	33	4.7	0	USGS
1983	11	30	74015	30.07	57.75	33	4.5	0	USGS
1984	4	20	114058	34.2	58.46	40	4.5	0	USGS
1984	8	6	111438	30.84	57.16	33	5.7	5.3	USGS
1984	8	14	13054	30.8	57.15	33	4.7	0	USGS
1984	8	15	20058	30.88	57.08	33	5.1	0	USGS
1984	10	23	70814	30.61	57.29	33	4.6	0	USGS
1985	3	3	135459	31.87	56.18	35	4.9	0	USGS
1985	5	21	3644	32.24	58.75	33	4.5	0	USGS
1985	6	28	133532	30.54	57.48	33	4.8	0	USGS
1985	12	9	132024	31.8	56	44	4.7	0	USGS
1985	12	13	15409	30.47	57.56	33	4.7	0	USGS
1985	12	23	234203	34.17	57.77	33	4.5	0	USGS
1986	3	27	114156	30.1	57.9	33	4.6	0	USGS
1986	4	10	120956	34.42	54.42	33	4	0	USGS
1987	2	23	112347	34.38	57.32	33	4.6	0	USGS
1987	4	2	95418	33.9	59.7	33	4.3	0	USGS
1987	4	11	23502	31.56	56.3	24	5	4.5	USGS
1987	4	22	10501	30.35	57.55	33	4.6	0	USGS
1987	7	20	164748	33.75	56.96	33	5	4.4	USGS
1987	8	30	55753	33.28	57.07	33	4.8	0	USGS
1988	4	13	34003	30.23	57.55	48	4.5	0	USGS
1988	5	8	65020	35.26	55.88	42	4.8	4	USGS
1988	5	27	205002	32.57	56.16	33	4.6	0	USGS
1988	10	13	172234	30.36	57.12	28	4.3	0	USGS
1988	11	9	124643	35.29	59.18	33	4.3	0	USGS
1988	12	3	12333	30.25	57.54	28	5.2	0	USGS
1989	1	17	233120	30.47	57.96	33	4.4	0	USGS
1989	6	23	154721	32.01	54.4	33	0	0	BISC

APPENDIX B

THE GENERAL DESCRIPTION AND INPUT PARAMETERS OF TELDYN

TELDYN is a computer program designed for equivalent linear, plane strain, and dynamic finite element analyses of soils and simple structures. In TELDYN, it is possible for the user to divide the input acceleration history into segments and the shear moduli and damping ratios are then set to be compatible with the average shear strains within each segment. Moreover, the excess pore pressures in saturated elements can be computed at the end of each segment and the shear moduli can then be determined in the next segment as a function of the reduced mean effective stress. The basic steps of input and output of TELDYN is given in the proceeding section briefly.

A. Input Data

1) Nodes

2) Elements

3) Boundary Conditions

   a) Compliant boundary

   b) Viscous boundary

   c) Mixed boundary

4) Materials Properties

   a) Material Curves

   b) Pore Pressure Generation Curves

   c) Specific Values of Material Parameters

d) Saturated Elements

5) Input motion

a) Data About Horizontal Input Motion

b) Data About Vertical Input Motion

B) Output Options

1) Print Options

2) Restart Options

The user can obtain the maximum accelerations and stresses in the system as output even after each iteration. Additionally the acceleration, shear stress or shear time histories for any node and element in the continuum can be obtained as output.

Appendix C

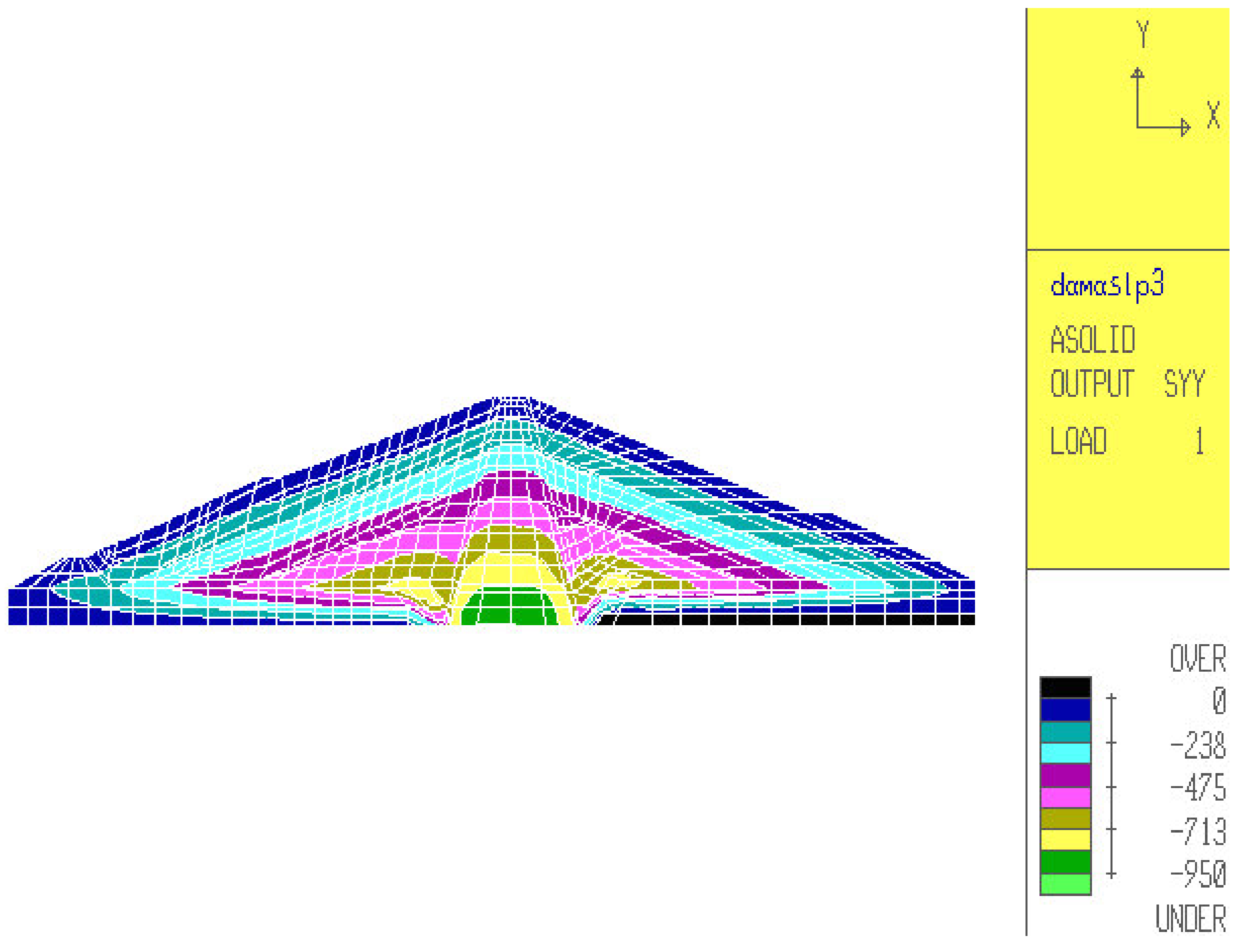
Y
X
damaslp3
ASOLID
OUTPUT SYY
LOAD 1
OVER
0
-238
-475
-713
-950
UNDER

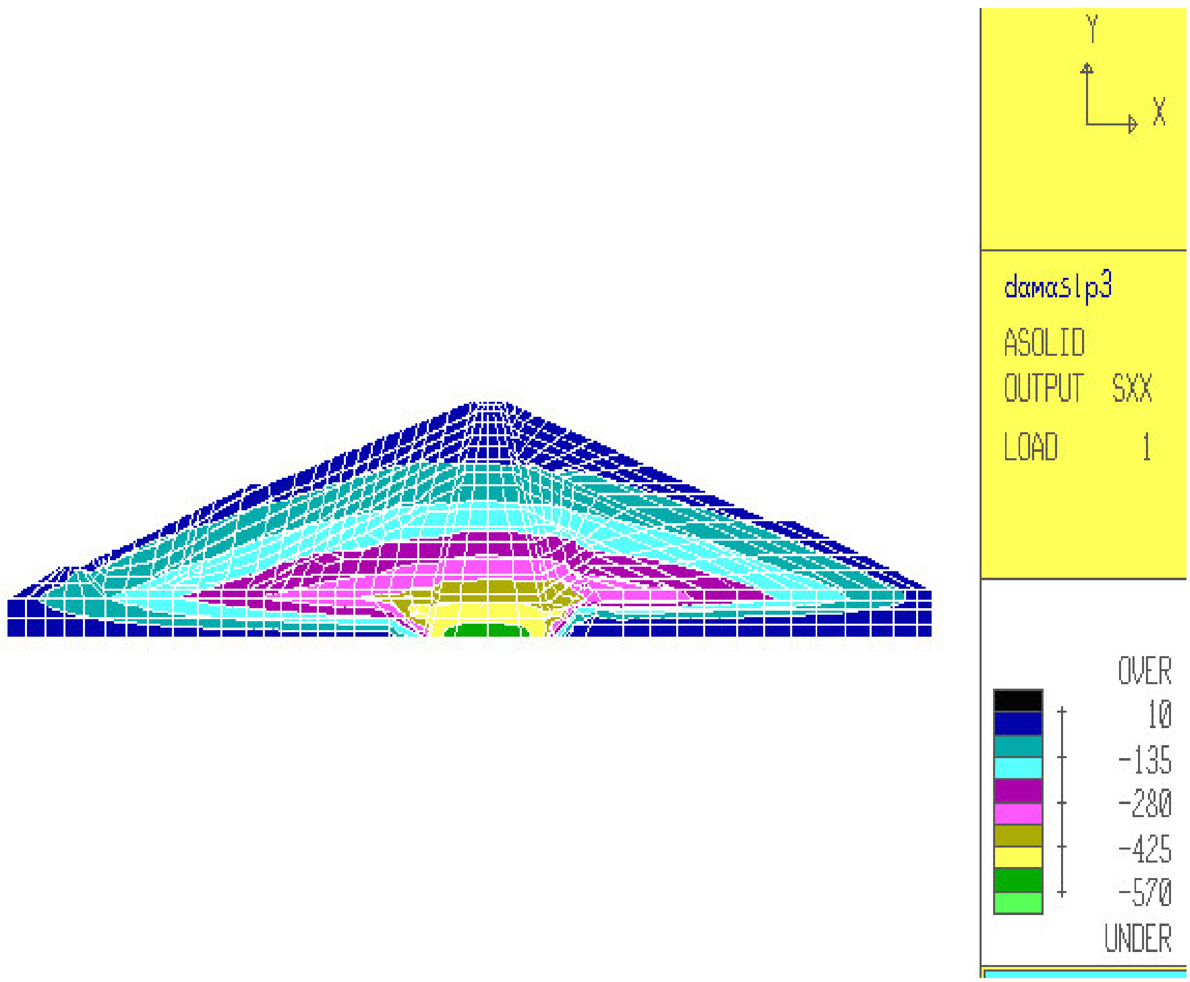
Y
X
damaslp3
ASOLID
OUTPUT SXX
LOAD 1
OVER
10
-135
-280
-425
-570
UNDER